Title

- Harmony COVID-19: a ready-to-use kit, low-cost detector, and smartphone app for point-of-care SARS-CoV-2 RNA detection
- Harmony COVID-19: point-of-care SARS-CoV-2 RNA detection

Authors

Nuttada Panpradist[1,2], Enos Kline[1], Robert G Atkinson[1], Michael Roller[1], Qin Wang[1], Ian T Hull[1], Jack H Kotnik[1,3], Amy K Oreskovic[1], Crissa Bennett[1], Daniel Leon[1], Victoria Lyon[3], Shane D Gilligan-Steinberg[1], Peter D Han[4,5], Paul K Drain[6], Lea M Starita[4,5], Matthew J Thompson[3], Barry R Lutz[1]*

AFFILIATIONS

1 Department of Bioengineering, University of Washington,
2 Global Health for Women, Adolescents, and Children, School of Public Health, University of Washington,
3 Department of Family Medicine, University of Washington,
4 Department of Genome Sciences, University of Washington,
5 Brotman Baty Institute for Precision Medicine,
6 Departments of Global Health, Medicine, and Epidemiology, University of Washington, Seattle, WA, USA

* **Corresponding author:** B. R. L. (blutz@uw.edu)
3720 15th Ave NE, Campus Box 355061, Seattle, Washington, United States 98195

Abstract (≤150 words)

RNA amplification tests sensitively detect SARS-CoV-2 infection, but their complexity and cost are prohibitive for expanding COVID-19 testing. We developed "Harmony COVID-19", a point-of-care test using inexpensive consumables, ready-to-use reagents, and a simple device accommodating up to 4 samples simultaneously. Our ready-to-use, multiplexed reverse-transcription, loop-mediated isothermal amplification (RT-LAMP) can detect down to 0.38 SARS-CoV-2 RNA copies/µL and can report in 17 min for high viral load samples (5,000 copies/µL). Harmony detected 97% or 83% of contrived samples with ≥0.5 viral particles/µL in nasal matrix or saliva, respectively. Evaluation in clinical nasal specimens in viral transport media (VTM, n=101) showed 100% detection of RNA extracted from specimens with ≥0.5 SARS-CoV-2 RNA copies/µL, with 100% specificity in specimens positive for other respiratory pathogens. VTM is non-ideal for Harmony system, yet extraction-free analysis (n=29) had 95% success in specimens with ≥1 RNA copies/µL. Usability testing performed first-time by healthcare workers showed 95% accuracy.

Teaser (≤125 characters with period)

A novel four-plexed RT-LAMP test kit operated by health workers can provide faster and more sensitive results than lab tests.

MAIN TEXT (11,642 words; limit 15,000 words)

Introduction

In 2019, an outbreak in China of SARS-CoV-2, the causative pathogen of COVID-19, rapidly became a global pandemic (*1*) and after a year it has infected 100 million

people and killed 2 million people (*2*). Multiple measures have been used to contain the spread of COVID-19. Governments imposed universal "stay-home" orders (*3*) to minimize transmission, which in turn has harmed mental health, social life, and the economy (*4*). Available vaccines do not completely prevent SARS-CoV-2 infections (*5*). Vaccinated individuals with breakthrough infections can transmit SARS-CoV-2 as much as unvaccinated individuals (*6*). Widespread COVID-19 testing and contact tracing is still a solution for sustained re-openings, allowing subsets of a community to resume work and begin to restore the economy. Moreover, testing is essential for the re-opening of international borders. Several countries have enforced a “fit-to-fly” policy; international travelers must test negative for COVID-19 within 72h before boarding international flights (*7*). Fast and sensitive point-of-care (**POC**) testing could facilitate the safe return to functioning domestic and international economies. POC testing could allow testing to expand to geographic regions that have limited access to centralized laboratory facilities, enable essential businesses to regularly test employees, and allow easy and efficient community testing by public health officials and clinics. Importantly, POC testing is critical in settings that require rapid turnaround time such as emergency urgent care facilities and points of introduction such as airports.

Here, we report the development of Harmony COVID-19 — a complete moderate-throughput sample-to-result system for sensitive POC detection of SARS-CoV-2 RNA. Harmony simplifies testing with ready-to-use assay reagents, an easy-to-use dedicated smartphone interface, and an inexpensive isothermal heater/detector device to enable POC testing. The assay includes three redundant SARS-CoV-2 targets to avoid false negatives due to viral mutation and an internal amplification control (**IAC**) in each test to avoid false negatives in case of assay failure. The heater/detector detects two-color real-time fluorescence for the SARS-CoV-2 redundant targets and IAC, and results are automatically reported on the smartphone. We evaluated the system using two panels of specimens - a panel of extracted nasal specimens from individuals with respiratory symptoms, and a panel of contrived specimens from the XPRIZE Rapid COVID Testing competition – and we conducted usability testing of Harmony by healthcare workers (**HCWs**). These evaluations have demonstrated that Harmony is a complete system for sample-to-result testing that is highly accurate in moderate complexity laboratories and clinic-based patient care settings.

RESULTS

Workflow and operation of COVID-19 Harmony

The Harmony test kit and detector were engineered for low-cost and simplicity of use to enable POC testing (**Fig. 1A**). The test involves taking a nasal swab, eluting the swab in a non-toxic buffer, and transferring the buffer to a reaction tube containing ready-to-use reagents. The reagent tube is inserted into the custom-designed heater/reader operated by a cell phone that provides instructions and displays the result. For samples with no target (**Fig. 1B**, left; NTC), detection of the IAC confirms that the reaction was functional; the absence of both target and IAC amplification indicates a failed reaction. For samples with SARS-CoV-2 RNA (**Fig. 1B**, middle; 200 copies/reaction, corresponding to 5 copies/µL), the green signal indicates a positive test, regardless of whether IAC is detected. Harmony using dry reagents detects down to 200 copies of SARS-CoV-2 RNA on a swab (**Fig. 1B**, right; 20

101 copies/reaction, corresponding to 0.5 copies/µL). Real-time detection reports a
102 positive sample as soon as the target signal appears, allowing detection in <30 min for
103 samples ≥2000 copies per swab (**Fig. 1C**), with earlier results for higher viral load.
104
105 **Novel modifications of RT-LAMP core assay chemistry**
106 The Harmony assay uses a unique variation of reverse transcription loop-mediated
107 isothermal amplification (**RT-LAMP**) that allows fluorescence detection of multiple
108 targets in the same reaction. The four-plexed assay amplifies three non-overlapping
109 genomic regions (**Fig. 1D**) of the SARS-CoV-2 nucleocapsid phosphoprotein (**N gene**)
110 reported by a green fluorescence signal (**FAM**) and an engineered **IAC** reported by a
111 red fluorescence signal (TEX 615 or Texas Red® - used interchangeably). A positive
112 test result is reported when any of the three SARS-CoV-2 targets are present. Presence
113 of IAC amplification is not necessary in a positive test. A negative test result is reported
114 if SARS-CoV-2 RNA is undetected, and the IAC is detected. If neither target nor IAC
115 is detected, it indicates a test failure, and the result is reported as indeterminate (**IND**).
116 Harmony primers target the SARS-CoV-2 N gene. Based on the initial design process
117 in early 2020, alignments of related coronaviruses (e.g., SARS-COV-1, MERS, bat
118 coronaviruses) confirmed that the N gene was likely to be a well-conserved target (not
119 the most conserved region) but was sufficiently divergent from related species to be
120 organism specific. At the time the sequence diversity of the virus was very low, thus
121 further SARS-CoV-2 specific analysis of the N gene by sequence analysis was not
122 possible. Therefore, primer design decisions were based on performance-driven
123 parameters such as computational estimates of primer properties (e.g., homodimers,
124 hairpin structures, Tm, %GC). Our recent *in-silico* analysis revealed that our primers
125 still have high coverage across new variants (*8*). The specific overlap with the U.S.
126 CDC primers (**Fig. 1D**) was semi-coincidental and possibly a consequence of shared
127 primer design requirements as suitable regions evaluated by analysis software, and the
128 small size of the N gene (1,275bp) relative to the footprint of our LAMP assays (213-
129 281bp). The proximity of our LAMP amplification targets on the same contiguous DNA
130 fragment may have an extra advantage to enable a synergistic initiation effect.
131 Amplification events could occur closely enough such that they could bump each other.
132 Other RT-LAMP technologies (**Table S1**) that amplify different genes would not
133 benefit from this effect. For the IAC amplification, we used a single LAMP loop primer
134 to intentionally impair the IAC amplification (**Table S2**) so that it would not
135 outcompete SARS-CoV-2 amplification.
136 Harmony also uses novel universal probes containing entirely engineered sequences
137 (*8*). The 5' FAM or 5'TEX 615 signal probes each have a 5' sequence region hybridized
138 to the complementary sequence region of its quencher probe that has 3' Iowa Black FQ
139 or 3' BHQ-2, respectively. In the absence of target or IAC amplification, these quencher
140 molecules remain proximal to their fluorophore pairs and absorb the fluorophore's
141 emission wavelengths. The signal probes each have a 3' overhang with a sequence
142 region identical to the 5' overhang of the loop primer for target or IAC. In the presence
143 of target or IAC amplification, quencher probes are displaced, enabling signal
144 detection.
145 To facilitate Harmony's multiplexed RT-LAMP, we employed newly developed,
146 strand displacing TFv1 chimeric DNA polymerase. Compared to the WarmStart Bst
147 DNA polymerase 2.0 commonly used in RT-LAMP SARS-CoV-2 assays (**Table S1)**,
148 (*9, 10*), TFv1 chimeric DNA polymerase has a comparable amplification rate in a
149 single-plex RT-LAMP (**Fig. 2A**) but a drastically faster amplification of SARS-CoV-
150 2 (**Fig. 2B**) and IAC targets in our four-plexed RT-LAMP (**Fig. 2C**).

151
152 **Ready-to-use reagents**
153 Our lyophilized RT-LAMP mixture contains primers, sequence-specific fluorescence
154 probes, IAC DNA template, polymerases, supporting proteins, and co-factors (**Fig.**
155 **3A**) and is activated by adding the nasal swab eluate containing additional buffer,
156 salts, and detergent. We initially screened excipient formulations that can
157 preserve enzymatic activity and do not significantly interfere with the primer or probe
158 behaviors. We selected trehalose and mannitol since they have been used as
159 excipients for PCR (*11-15*) and LAMP (*16*). We found that mannitol did not
160 drastically impact the Harmony's sensitivity compared to trehalose at the same
161 concentration (**Fig. S1**) and did not require adjusting the reaction temperature to
162 maintain the assay speed. Possibly, this is due to the effect of trehalose on altering
163 primer and probe melting temperatures (*17*).
164 Using a commercial real-time thermal cycler, lyophilized RT-LAMP detected 3/3
165 replicates of 15 RNA copies/reaction (0.38 copies/µL), and IAC was detected in all
166 negative samples (**Fig. 3B**). RT-LAMP amplification of 2 x 10^5 RNA copies/reaction
167 using the dry reagents generated detectable signal in 17 min (**Fig. 3C**). We subsequently
168 tested our in-house lyophilized reagents on a larger number of technical replicates of
169 SARS-CoV-2 RNA at 20 copies/reaction (0.5 copies/µL) using multiple batches, and
170 90% (36/40, 95% confidence interval (**CI**): 76 - 97%) were amplified (**Fig. 3D**).
171 Medians of time to detection for FAM and TEX 615 signals were 28.6 min (range: 28.0
172 - 29.4) and 31.7 min (range: 31.1 - 32.7), respectively. Based on these preliminary
173 experiments, our limit of detection (**LOD**) is 15-20 copies/reaction (0.38 - 0.5
174 copies/µL) when analyzing purified, synthetic SARS-CoV-2 RNA. Next, we tested our
175 lyophilized RT-LAMP reactions with simulated nasal matrix (salt, mucin, human
176 DNA) to mimic human nasal samples. We observed a 10-min delay in amplification of
177 both SARS-CoV-2 RNA and IAC DNA (**Fig. 3E**), but all targets were detected
178 correctly. Greater interference or other harm to the reaction will further delay IAC
179 amplification; thus, the IAC serves as an indicator of the reaction's function and can
180 prevent reporting false negatives due to interference or damaged reagents. By setting a
181 60-min reaction time, the assay can suffer some delay while still correctly identifying
182 positive samples. Specificity testing against closely related pathogens MERS and
183 SARS-CoV-1 showed no cross-reactivity (**Fig. S2**).
184
185 **Hardware: housing and real-time fluorescence reader device**
186 The Harmony system includes a heater/detector device controlled by a dedicated cell
187 phone and plastic housing with a sample setup station (**Fig. 4A**). The heater/detector
188 device (**Fig. 4B**) includes an aluminum heater block with four wells and a spring-
189 loaded heated lid to prevent condensation. A proportional integral derivative (**PID**)
190 feedback loop running on a microcontroller allows recovery of the temperature
191 setpoint within 3-4 min after disturbance from opening the lid (**Fig. 4C**). Two LEDs
192 (**Fig. 4D**) provide the excitation light by shining down through the top of each sample
193 tube. Fluorescence emission passes through holes drilled on the side of the heater
194 block. Each sample well has an emission filter/photodiode set on each side to detect
195 two emission wavelengths (**Fig. 4E**). A blue LED (dominant wavelength 470nm) is
196 used to excite FAM, and the emission photodiode sits behind a dielectric 550nm
197 longpass filter. A yellow LED (dominant wavelength 587nm) is used to excite TEX
198 615, and a second emission photodiode sits behind a 630nm longpass dielectric filter.
199

Thermostable Inorganic Pyrophosphatase enables real-time LAMP detection in the Harmony COVID-19 device

RT-LAMP generates inorganic pyrophosphates (**PPi**) that precipitate from the solution. The cloudiness created by precipitates has been used as a visual readout signal for LAMP (*18*), but here the cloudiness scattered light and caused non-specific signals in NTC samples (**Fig. 4F,** top) when tested on device. Inorganic pyrophosphatase (**TiPP**) can be added to the LAMP reaction to hydrolyze built-up pyrophosphate, and this combination has been used in other contexts to improve differentiation of LAMP products in melt analysis (*19*) and indirectly detect LAMP via phosphate ions hydrolyzed by the TiPP (*20*). In fact, TiPP was advertised for its use for the enhancement of DNA replication (*21*), mitigating pyrophosphorolysis during DNA synthesis for sequencing (*22*). In our context, we added TiPP in the RT-LAMP reaction to eliminate scattered signal from pyrophosphate to prevent non-specific signal in negative reactions (**Fig. 4F,** bottom). Interestingly, this effect was not observed when the reaction was tested in the commercial thermal cycler (BioRad CFX96). This is potentially because the commercial thermal cycler uses bandpass filters for both excitation and emission wavelengths, while our device does not have excitation filters.

In addition to the physical effects, we have postulated that PPi accumulation may inhibit LAMP; as PPi forms, magnesium phosphate precipitate, Mg^{2+}, will be sequestered from the reaction, potentially impairing polymerase activity and primer hybridization. TiPP addition reduces the turbidity that is indicative of magnesium phosphate precipitate, so it may limit the depletion of reaction components. This has implications for multiplexed LAMP reactions, where concurrent amplification of multiple targets is a desired outcome. This possibility or the specific capability of TiPP to "enhance" LAMP has not yet been evaluated.

Multi-purpose Android mobile app: instruction, temperature control, and real-time analysis of results

The phone software provides interactive guidance for setting up the test. It prompts the user to input a sample ID by scanning a barcode, capturing a photo, or typing a sample ID (**Fig. 5, A-D**). The software also carries out the closed-loop temperature control for the heater block and lid heater, and it displays the status of the heater block to prompt the user to insert the reaction tubes only after the heater reaches the reaction temperature (**Fig. 5E)**. During the test run, the screen displays the test status ("analysis in progress") and elapsed time, or it reports any detected errors ("failed run") (**Fig. 5F**). Importantly, the software performs real-time data analysis that detects fluorescence intensity rise above a dynamically and automatically computed background level. Signals from SARS-CoV-2 can appear early in the test, especially for high viral loads, and the real-time analysis allows reporting of positive tests immediately after they are detected (**Fig. 5G**). Negative results and IND results are reported at the end of the test run time (**Fig. 5H**). Software analysis is described in the Methods section.

Evaluation Harmony COVID-19 system on contrived SARS-CoV-2 samples (XPRIZE panel) without extraction

A panel of contrived samples from the COVID-19 XPRIZE competition were tested on the Harmony system. For SARS-CoV-2 virus in 1xPBS (**Fig. 6A**), Harmony detected all positive samples containing ≥50 SARS-CoV-2 viral particles/rxn, and 96% of samples containing ≥20 viral particles/rxn. In human nasal matrix (**Fig. 6B**)

250 and human saliva (**Fig. 6C**), Harmony detected 97% and 83%, respectively, of
251 samples containing ≥20 viral particles/rxn. Harmony had zero false positives across
252 all sample types. Interestingly, unlike the case of simulated nasal matrix (**Fig. 3E**), we
253 did not observe delayed detection time of IAC in human nasal or saliva samples.
254 Detection times (mean ± SD) for IAC amplification in negative samples were 32.9 ±
255 3.8 min for PBS, 35.8 ± 4.8 min for human nasal matrix, and 34.3 ± 11 min for human
256 saliva, respectively ($p>0.05$; t-test, two-tailed). It is worth noting that in this
257 experiment RT-LAMP reactions were either set up at room temperature (intended
258 protocol for our assay, hollow symbols) or on ice (protocol used by most EUA RT-
259 LAMP assays as summarized in **Table S1**, solid symbols). Even with a small sample
260 size, we observed relatively delayed reaction and more false negative results when the
261 reaction was set up on ice, especially those near the LoD (*i.e.*, 20 copies/rxn).
262
263 **Evaluation of clinical specimens using the Harmony COVID-19 system**
264 We first tested the assay for reactivity with SARS-CoV-2 and cross-reactivity with
265 other respiratory pathogens using RNA extracted from infected patient specimens.
266 The retrospective clinical samples had been collected in viral transport medium
267 (VTM), which is not the intended sample type for Harmony, since a POC test uses
268 fresh samples and does not require sample transport. Subsequently, we tested a
269 smaller panel enriched with positive specimens to assess the feasibility of detecting
270 SARS-CoV-2 RNA in VTM specimens without extraction.
271 Clinical VTM specimens were collected from individuals positive for SARS-CoV-2
272 (*n = 33*) or for other pathogenic respiratory infections (*n = 68*) and were re-tested by
273 RT-qPCR using CDC primer and probe sequences (*23*) to measure the SARS-CoV-2
274 viral load and provide the reference test result. Using RT-qPCR with CDC
275 primers/probes, 68 specimens were confirmed to be SARS-CoV-2 negative (**Fig. 7A,**
276 **left**), 30 specimens were confirmed to be SARS-CoV-2 positive (**Fig. 7A, right**), and
277 three previously positive specimens were only detected by one RT-qPCR assay (either
278 N1 or N2) and classified as inconclusive (**INC, Fig. 7A,** middle).
279 Specimens were tested in duplicate on Harmony using the ready-to-use reagents (**Fig.**
280 **7A)**, amplification curves are arranged from low to high virus concentration as
281 quantified by RT-qPCR assay (**Fig. S8** and **Fig. S9**). Out of 30 RT-qPCR-positive
282 specimens, Harmony detected 26 specimens in both technical replicates and 3
283 specimens in one of the two replicates. In the three RT-qPCR INC results, one sample
284 was detected by Harmony in one of the two replicates. Excluding the RT-qPCR INC
285 specimens and applying a stringent requirement for both Harmony replicates to be
286 detected to report a positive test, Harmony achieved 96% accuracy (94/98, 95%CI:
287 88-98%), 87% sensitivity (26/30, 95%CI: 69-96%), and 100% specificity (68/68,
288 95%CI: 94-100%). If replicates are treated independently (**Fig. 7B**), Harmony
289 detected 55/60 positive specimens (92% sensitivity, 95%CI: 82-97%). Harmony
290 detected all positive specimens with ≥20 copies/reaction (0.5 copies/μL). The clinical
291 panel (**Fig. 7A**) included 68 specimens that were SARS-CoV-2 negative but contained
292 other respiratory pathogens including influenza, rhinovirus, and seasonal coronavirus
293 (**Fig. 7C**), as determined using OpenArray (a laboratory PCR test with microarray
294 detection) (*24*). Harmony correctly identified all SARS-CoV-2 negative specimens
295 (**Fig. 7A,** left). **Fig. 7B** summarizes the performance of Harmony on detecting
296 extracted RNA from clinical VTM specimens.
297 Next, we used Harmony to detect SARS-CoV-2 in VTM specimens without RNA
298 extraction. We expected the presence of microbial agents in the VTM to delay
299 amplification and thus we ran the reaction for additional 30 min. Compared to RT-

qPCR, Harmony with 90-min run time detected 18/24 positive specimens in both replicates and 3/24 in one of the replicates. Considering each replicate independently, Harmony detected 78% (32/41) and 95% (39/41) SARS-CoV-2 RNA positive specimens within 60- and 90-min detection time, respectively. Detection time (mean ± SD) of IAC in the negative samples with direct VTM amplification (43.9 ± 6.4 min) was significantly slower than the detection time with extracted RNA (38.5 ± 1.6 min; p=0.03, t-test, two-tailed). Pair-wise comparison among positive SARS-CoV-2 specimens (**Fig. 7E**) showed two specimens with significantly different detection time. Even though VTM is not the intended sample type, Harmony detected 95% of SARS-CoV-2 VTM specimens that contained at least 1 copy/µL (**Fig. 7F)**.

Feasibility testing: sample-to-result system tested by healthcare workers and laboratory personnel

To complete the system, we developed a test kit that included all components needed for running a test, including the swab, elution buffer, a fluid transfer device, and a ready-to-use reagent tube. Swabs were pre-loaded with SARS-CoV-2 DNA to serve as a control sample to evaluate performance by HCWs and laboratory personnel (**LPs**).

In the first phase of user testing (**Fig. 8A**), we compared the accuracy and reproducibility of two methods for transferring the eluate to the reaction tube when operated by LPs *(n = 5*) and HCWs (such as nurses, medical students, and dental students; *n = 10*). The first method (**Fig. 8B** and shown-previously in **Fig. 1**) used a unified sampler-dispenser. The second method (**Fig. 8C**) used a transfer pipette to transfer a fixed volume of fluid to the reaction tube. Regardless of the baseline skill of operators, transfer pipettes yielded more reproducible recovered volumes than the unified dispenser (F-test, p <0.001). Recovered volumes of the two methods were not significantly different between HCWs and LPs (student's t-test, two-sided, p = 0.90; **Fig. 8D**). User feedback on the transfer methods and preferences on tube sizes are summarized in **Table S3**. Next, HCWs and LPs executed the full Harmony workflow on contrived SARS-CoV-2 DNA swab samples (**Fig. 8**). Using the transfer pipette workflow (**Fig. 8E**), the test accuracy was 100% (10/10) for LPs and 95% (19/20) for HCWs. Surprisingly, we found that the HCWs performed better than the LPs when using the unified dispenser system (**Fig. 8F**) when considering both accuracy and IND rates. HCWs had significantly lower (Z-test, two-tailed, p<0.05) IND results (1/20) than LPs (3/10) when using the unified dispenser system. Excluding IND results, the HCWs had 89% accuracy, higher than LPs with 71% accuracy (Z-test, two-tailed, p <0.05), when using the unified dispenser system.

Discussion

This work presents a combination of multi-disciplinary engineering (molecular, mechanical, electrical, software, human interface design) to develop a complete system for SARS-CoV-2 detection at the POC. The system is inexpensive and simple yet has features comparable to laboratory-based tests (**Table 1A**). The assay has high sensitivity and specificity in clinical and contrived specimens, and HCWs successfully performed the workflow with high accuracy.

Harmony uses ready-to-use reagents that enable fast and accurate assay setup while maintaining high assay sensitivity and specificity. The lyophilized Harmony assay detected as low as 15 copies/reaction of synthetic SARS-CoV-2 RNA and detected all

347 extracted RNA from clinical specimens at ≥20 copies/reaction with no false positives
348 across all sample types. Harmony chemistry is also robust, enabling detection of
349 contrived samples in human nasal matrix (intended sample type) and saliva without
350 RNA extraction. We found excellent sensitivity when testing samples with ≥20 viral
351 particles in nasal matrix (estimated 500 copies/swab for 1mL elution buffer and 40µL
352 reaction). In saliva samples at the same concentrations (not the intended sample type),
353 Harmony showed moderate sensitivity. Heat treatment of saliva shown to enable
354 detection by RT-PCR (*25*) would likely improve the sensitivity of Harmony with saliva
355 samples. Regardless, our current level of assay sensitivity would be sufficient to detect
356 SARS-CoV-2 in most nasal specimens (~10^3 to ~10^9 copies/swab) (*26*) or saliva (~10^4
357 to ~10^8 copies/mL) (*27*) from infected individuals during the first week after the onset.

358 Harmony's high assay sensitivity and specificity despite its high multiplexity was made
359 possible by multiple modifications to traditional RT-LAMP. We used novel polymerase
360 and probe design that can specifically discriminate between the SARS-CoV-2 from
361 IAC amplification while most RT-LAMP analysis in tube relies on detection of total
362 amplification and split each RT-LAMP reaction to detect only one target/reaction
363 (**Table S1**). Multi-target amplification is essential to reduce false negatives in SARS-
364 CoV-2 nucleic acid tests as the new variants continue to emerge.

365 In addition to the core assay, our lyophilization process also involves non-traditional
366 modifications. Unlike other lyophilized RT-LAMP (*28*), our lyophilized reagents are
367 magnesium-free, which prohibits any enzymatic activity that may occur before assay
368 initiation. Our lyophilized RT-LAMP is activated upon the addition of sample which
369 contains magnesium and detergent. Thus, it should be less prone to moisture
370 degradation than magnesium-containing lyophilized RT-LAMP. Secondly, RT-
371 WarmStart enzyme in Harmony assay is inactive at room-temperature and thus
372 prevented activities during the reaction set up and eliminated the need for setting up the
373 reaction on ice as performed in other SARS-CoV-2 LAMP assays (**Table S1**). Cold
374 temperature can promote dimer and/or secondary structures of LAMP primers, which
375 we observed as a negative impact on the assay sensitivity and speed. In fact, while
376 setting up Harmony assay for lyophilization, RT-LAMP primers and probes were
377 heated and cooled down passively at room temperature to minimize secondary
378 structures prior to mixing with the other components. Last, we removed water to reduce
379 the final volume of lyophilized reaction to 20µL. This enabled doubling the excipient
380 concentrations in the lyophilized pellet and shortens the lyophilization drying time.
381 When testing samples, the excipients are then diluted by half to 40µL reaction, thus
382 reducing any impact of excipients on the core assay function. We anticipate that these
383 components will be stable up to 30 °C but future experiments will be conducted in the
384 final form of the product for future commercialization efforts.

385 Isothermal amplification, like RT-LAMP in Harmony, is often promoted as ideal for
386 POC testing because it can be carried out using a constant temperature heat source,
387 such as a water bath, heat block, or even more novel sources (chemical heat source,
388 sunlight, body temperature) (*29*). However, reported tests often have other limitations
389 that may prevent their use in POC testing (**Table 1B**). Common limitations include
390 use of frozen reagent stocks that must be thawed and then formulated using laboratory
391 pipettes, manual steps for sample processing that require laboratory skill, or detection
392 steps that rely heavily on user interpretation or analysis by a user's cell phone.
393 Harmony is a complete sample-to-result system that uses ready-to-use reagents for
394 simple 1-minute setup and a dedicated device that reports results without extra post-
395 amplification steps or reliance on user interpretation.

Some RT-LAMP tests use end-point lateral flow strips for detection (**Table S1**), which adds a user step, but more importantly, should not be done at the POC because it exposes the testing site to amplicons that will give false positive results in subsequent tests. Others use in-tube detection by eye (*30*) or a cell phone (*31*) which increases the user burden and could introduce additional sources of error. Real-time detection used in Harmony COVID-19 removes the need for extra detection steps or user interpretation. Real-time detection also allows Harmony to report positive results as soon as the SARS-CoV-2 signal appears rather than waiting for an end-point detection method. High viral load samples could be detected in as little as 20 min, which could enable more timely infection control measures to limit viral spread. Harmony real-time detection allows testing without opening tubes after amplification, requires no extra steps or interpretation by the user, and allows reporting a positive sample earlier than end-point detection methods.

The Harmony device automates heating, multiplexed detection, and data interpretation. We integrated a simple heater with low-cost LEDs and sensors to enable real-time two-color detection of RT-LAMP fluorescence in four independent sample wells. The device costs <US$300 in parts for prototypes, while the lowest cost of a commercial RT-PCR machine on the market is >US$5000(*32*). Moreover, the Harmony device is portable and energy-efficient, requiring <15 watts and operable by USB power sources. These features are attractive for use at the POC in the U.S. and resource-limited settings.

Lastly, the simple workflow and analysis of Harmony is appropriate for POC testing. Test operation involves a few simple steps that take ~1 minute, and there are no further user steps after starting the test. Here, HCWs were able to operate the tests with simple written instructions and a video showing the procedures. The simplicity of the Harmony procedure and completeness of the stand-alone system can be a significant advantage for onboarding to ambulatory care settings and potentially community testing locations. Compared to existing US FDA EUA RT-LAMP tests (**Table S1**), Harmony is very competitive. Most RT-LAMP technologies are not designed for use in CLIA-waived settings. Lucira™ is the only product approved for use at the POC, but it is custom-designed to be battery-powered and completely disposable. This strategy, while is convenient for users, can contribute to electronic waste and relatively high cost for producing a unit. In contrast, Harmony relies on low-cost consumables and generates no electronic waste after each run.

In this study, we evaluated the system using contrived specimens in nasal and saliva matrix (XPRIZE) and clinical specimens stored in VTM, which may not reflect the performance in fresh clinical samples. These samples were used due to the difficulty of obtaining fresh dry swabs intended for this POC test. Because VTM is irrelevant for immediate testing at the POC, we tested RNA extracted from clinical samples to assess the overall assay performance on clinical RNA and subsequently tested feasibility of direct amplification of VTM samples. Nevertheless, this testing shows excellent analytical reactivity to clinical specimens, no cross-reactivity with other respiratory pathogens, analytical sensitivity comparable to the CDC RT-PCR, and resilience in the presence of nasal matrix. While our assay is relatively fast and sensitive, there is potential to further improve the performance. We ran RT-LAMP at 64°C, which is 9°C above the optimal temperature for the RT enzyme. We hypothesize that cooling of the heat block when the lid is open, followed by a few minutes to ramp back up to 64°C, provided an opportunity for the RT enzyme to operate. In contrast, the reaction speed of the temperature-stable TFv1 DNA

445 polymerase in this assay is optimal at higher temperature. Thus, operating the device
446 with an initial 55°C step for optimal RT activity followed by a higher temperature
447 step for fast DNA amplification could increase sensitivity and/or speed.

448 The current design of RT-LAMP assay can be improved to include an IAC that is
449 more representative of the SARS-CoV-2 virus. We currently use a DNA IAC, which
450 has been used in several EUA assays, but the DNA control does not capture the
451 potential failure of the lysis and cDNA conversion processes. We are developing a
452 new IAC that uses RNA that can be packaged in a viral envelope. This modification
453 may require re-development of excipients that preserve the RT-LAMP enzymes and
454 the enveloped RNA.

455 POC tests like Harmony could provide rapid testing to enable the re-opening of
456 businesses, schools, and borders; but the need for POC testing extends beyond the
457 current emergency. As natural immunity and vaccination take hold, COVID-19 is
458 likely to become endemic with seasonal outbreaks. Tests such as Harmony will be
459 necessary not only to help identify individuals with SARS-CoV-2, but other
460 respiratory pathogens such as influenza and RSV, as the symptoms of these are
461 similar. Prior to the current SARS-CoV-2 pandemic, the yearly influenza infections
462 caused nearly 30 million cases in the U.S. alone, with 400,000 hospital admission and
463 35,000 deaths (*33, 34*). Indeed, particularly when more typical patterns of respiratory
464 infections occur, there will be a need for tests that can perform multiplex testing for
465 individuals presenting respiratory symptoms. Tests such as Harmony will become a
466 common practice for confirming presence of viral infections that can be treated with
467 antiviral therapies or that demand infection control, as well as helping to reduce
468 inappropriate use of antibiotics. Further, test platforms developed for this pandemic
469 could be more readily adapted to detect new diseases to increase readiness for future
470 pandemics. The advances in awareness and acceptance of testing for infections at
471 scale, and the technology platforms developed will have an ongoing benefit for
472 COVID-19 control, reducing harm from other endemic diseases, and fighting future
473 pandemics.

474 **Materials and Methods**

475 **Preparation of synthetic RNA standards**
476 MERS and SARS-CoV-1 plasmid standards (10006623 and 10006624, Integrated
477 DNA Technologies, Coralville, IA) were amplified using M13 PCR primers to
478 generate DNA templates tagged with T7 promoter sequences. DNA templates
479 containing T7 promoter sequences were transcribed using Hi-T7 RNA polymerase
480 (M0658, New England Biolabs, Lawley, MA) following the manufacturer's protocol,
481 with 1 U/µL RNase inhibitor (N2611, Promega, Madison, WI) added. Following
482 transcription, 0.01U/µL DNase I (EN0521, ThermoFisher Scientific, Waltham, MA)
483 was added to each reaction, and incubated at 37°C for 15 min. RNA transcripts were
484 purified with Monarch RNA Cleanup Kits (T2040, New England Biolabs). RNA was
485 quantified on a Qubit 4 fluorometer (Q32852, RNA HS Assay Kit, ThermoFisher
486 Scientific, Waltham, MA), and checked for length and integrity by electrophoresis on
487 a 2200 TapeStation (5067 RNA ScreenTape, Agilent Technologies, Santa Clara, CA).
488 RNA at 10^{10} copies/µL was stored in nuclease-free water in single-use aliquots.
489 SARS-CoV-2 RNA was prepared and quantified as previously described (*35, 36*).
490
491 **In-house TFv1 polymerase production**

492 **Plasmid preparation:** The chimeric polymerase (TFv1) was generated by assembly
493 PCR using genomic material from *Thermus thermophilus* (*T. th*) HB27 (ATCC BAA-
494 163D-5™, Gaithersburg, MD) and a synthetic gene fragment derived from
495 *Thermodesulfatator indicus* (*T. in*), (Integrated DNA Technologies, Coralville, IA),
496 similar to the method previously described (*37*). Briefly, a 3' terminal fragment of the
497 *T. th* HB27 *polA* gene downstream of the finger domain was amplified by PCR using
498 Phusion® Hot Start Flex DNA Polymerase (M0535L, New England Biolabs) with a
499 modified forward primer containing sequence overlap with the *T. in polA* gene
500 fragment *(AA734-795,* codon optimized for *E. coli)*. A chimeric sequence was then
501 generated by assembly PCR. A second *T. th* polymerase fragment, upstream of the
502 finger domain and lacking the 3'to 5' exonuclease domains, was similarly amplified
503 and appended to the 5' end of the chimeric fragment. The resultant sequence
504 corresponds to a *T. th* DNA polymerase I fragment, orthologous to the Stoffel
505 fragment of *T. aq* polymerase, with a replacement in the finger domain derived from
506 *T. in*. This gene was then cloned into the expression vector pET His6 TEV LIC
507 cloning vector (2B-T) (a gift from Scott Gradia, Plasmid # 29666, Addgene,
508 Watertown, MA) by ligation independent cloning (*38*). The annealed vector and insert
509 were transformed into T7 Express lysY/Iq Competent *E. coli* (C2987H, New England
510 Biolabs) per the manufacturer's protocol and plated on LB 100µg/mL carbenicillin
511 plates. Colony plasmid inserts were verified by Sanger sequencing.
512 **Protein expression and purification:** 50mL starter culture in LB broth with
513 100µg/mL carbenicillin was inoculated with a sequence-verified colony and incubated
514 at 30°C overnight in a shaking incubator at 200rpm. The culture was centrifuged at
515 5,000 RCF for 15 min and resuspended in an equivalent volume fresh LB
516 carbenicillin media. Flasks of 500mL LB broth with 100µg/mL carbenicillin were
517 inoculated with 5mL each of resuspended starter culture and incubated at 37°C in a
518 shaking incubator at 200rpm until OD_{600} of 0.4-0.6 had been achieved. Cultures were
519 induced with 0.4mg/mL of IPTG and incubated for two hours then harvested by
520 centrifugation at 5,000 RCF for 15 min, decanted, and stored as cell pellets at –80°C
521 until needed. Prior to purification, cell pellets were resuspended in lysis buffer (20mM
522 sodium phosphate pH 7.4, 80mM NaCl, 1% *(v/v)* Triton (648466 Sigma, St. Louis,
523 MO), and 1mg/mL lysozyme from chicken egg white (Millipore Sigma, Burlington,
524 MA)). Suspensions were heated at 37°C for 20 min, then lysed by ultrasonic
525 disruption using a Fisherbrand™ Model 120 Sonic Dismembrator (Fisher Scientific,
526 Waltham, MA) with two cycles of two-second pulses at 50% amplitude for 2 min,
527 while on ice. Lysates were heat-clarified at 65°C for 20 min, followed by
528 centrifugation at 20,000 RCF. The supernatant was collected and diluted with sample
529 diluent buffer (20mM sodium phosphate, 1.8M NaCI, pH 7.4 for 6x stock; 5 parts
530 supernatant to 1 part diluent buffer) and filtered with a 0.22 µm syringe filter (25-342
531 Olympus, Genesee Scientific, San Diego, CA). The purified clarified lysate was
532 applied to a 1mL Hitrap Talon Crude column (Cytiva, Marlborough, MA) and
533 enriched per manufacturer's default recommended specifications using an ÄKTA start
534 system with the Frac30 fraction collector (Cytiva). Elution fractions were evaluated
535 by A_{280} on a spectrophotometer (2200 Nanodrop, Fisher Scientific) using the protein's
536 expected molecular weight (63.062 kDa) and extinction coefficient (60,850 m^2/mol)
537 of the His-tagged polymerase. Elution fractions containing protein were diluted 1:10
538 with 10mM sodium phosphate and applied to a 1mL HiTrap® Heparin HP column and
539 purified per the manufacturer's recommended specifications except for a modified
540 binding buffer (10mM sodium phosphate and 30mM NaCl at pH 7). Fractions
541 containing protein were concentrated and buffer exchanged into storage buffer

542 (17mM Tris-HCI, 167mM KCI, 17% glycerol, pH 7.5) using an Amicon® Ultra-2
543 30K centrifugal filter (Millipore Sigma), as recommended by the manufacturer. The
544 recovered polymerase solution was then adjusted to 10mM Tris-HCI, 100mM KCI,
545 2mM DTT, 0.1% Triton X-100, 50% glycerol, pH 7.5. Polymerase purity was
546 evaluated by SDS-PAGE and spectrophotometry throughout purification.

547

548 **RT-LAMP assay design**

549 Alignment of SARS-CoV-2 sequences (available on NCBI up to January 2020) were
550 performed using Geneious (Auckland, New Zealand). Three sets of LAMP primers
551 (Harmony NC1, Harmony NC2, and Harmony NC3) were developed targeting the
552 22,285 – 28,517 (232 bases), 28,528 – 28,471 (213 bases), and 29,135 – 29,416 (281
553 bases) regions of the SARS-CoV-2 nucleocapsid phosphoprotein gene. *In silico*
554 analysis showed that this primer design matched 100% of SARS-CoV-2 sequences
555 and did not have cross-reactivity to MERS and SARS-CoV-1. We used two detection
556 probes, each comprised of a fluorescent probe and its complementary quencher probe.
557 For detection of SARS-CoV-2 RNA amplification, we used FAM labeled detection
558 probe and Iowa Black™ quencher probe. For detection of IAC amplification, we used
559 TEX 615 labeled detection probe and BHQ2 labeled quencher probe. The primer and
560 probe sequences are listed in T**able S2**.

561

562 **Wet RT-LAMP reactions**

563 Characterization of polymerases (**Fig. 2**) was conducted in the wet reaction format.
564 2µL water or SARS-CoV-2 RNA at 200 or 2000 copies/µL was added to 38µL master
565 mix to achieve a 40µL RT-LAMP reaction. 20x Harmony NC1, NC2, and NC3
566 primer mix for SARS-CoV-2 amplification each contained 20µM each FIP/BIP
567 primer, 10µM each loop primer, and 4µM each F3/B3 primer. 20x IAC primer stock
568 contained 10µM loop primer. 20x probe/quencher mix for SARS-CoV-2 or IAC
569 amplification contained 4µM fluorophore probes and 6µM quencher probes).
570 Depending on the experimental design, each RT-LAMP reaction contained 1x each
571 primer mix or only 1x NC1 primer mix, 1x each probe or only 1x FAM probe, 2.5%
572 (*v/v*) mannitol (OPS Diagnostics EXMN 500-01), 5mM DTT, 0.6U/µL WarmStart
573 RTx, 0.7µg TFv1 DNA polymerase or 0.32U/µL Warmstart DNA polymerase 2.0 (M
574 0538, New England Biolabs), 1.4mM each dNTP, 1U/µL RNase inhibitor (N2615,
575 Promega), 25mU/µL thermostable inorganic pyrophosphatase (M0296L, New
576 England Biolabs), 250 copies/µL IAC DNA, 6mM magnesium sulfate, 1x ThermoPol
577 buffer (B9004S, New England Biolabs) in nuclease-free water. RT-LAMP reactions
578 were incubated at 63.3°C and FAM and/or Texas Red signal was read every 13s for
579 1h using a CFX96 thermal cycler (Bio-Rad).

580

581 **Lyophilization of RT-LAMP reagents**

582 Reactions containing 2x primers (2µM each FIP/BIP primer, 1µM each loop primer,
583 and 0.4µM each F3/B3 primer) and probes (0.4µM fluorophore probes and 0.6µM
584 quencher probes) in the presence of 5% *(v/v)* mannitol, 10mM DTT, 1.4µg TFv1
585 DNA polymerase, 1.2U/µL WarmStart RTx, 2.8mM each dNTP in 10mM Tris-HCl,
586 pH 7.4, 2U/µL RNase inhibitor, 50mU/µL thermostable inorganic pyrophosphatase,
587 and 500 copies/µL IAC DNA were prepared in 20µL aliquots of 0.2mL reagent tubes
588 and lyophilized. Packages were stored in desiccant packets at -20°C until use.

589

590 **Harmony RT-LAMP reaction setup**

591 Lyophilized reagents were resuspended in a final volume of 40µL containing 1x
592 rehydration buffer (1x ThermoPol buffer (B9004S, New England Biolabs), 6mM
593 supplemental $MgSO_4$, and 0.5% *(v/v)* Triton X-100). For analytical sensitivity
594 experiments, 2µL SARS-CoV-2 RNA in water was added. For clinical testing, 10µL
595 extracted RNA was added to each RT-LAMP reaction. For testing the XPRIZE
596 contrived specimens or VTM in direct-to-amplification experiments, 10µL sample
597 (not extracted) was added to each RT-LAMP reaction. For usability testing, 40µL
598 swab eluate was added directly to the RT-LAMP reaction using transfer pipettes or
599 the in-house unified dispensers.
600
601 **Analytical sensitivity of RT-LAMP assay**
602 Analytical sensitivity of lyophilized RT-LAMP was tested using purified RNA (0-
603 $2x10^6$ copies/40µL reaction). We also tested the effect of salt, human DNA, and
604 mucin on amplification of SARS-CoV-2 RNA and IAC DNA using simulated nasal
605 matrix as previously described (*39*).
606
607 **Preparation of contrived swab samples and kits for usability testing**
608 For the transfer pipette workflow, each kit contained one swab (either positive or
609 negative), a vial (10-500-25, Fisher Scientific, Waltham, MA) containing 400µL of 1x
610 rehydration buffer (see section RT-LAMP reaction setup), and one lyophilized RT-
611 LAMP reagent tube. For positive swabs, 10µL of 100 copies/µL SARS-CoV-2 DNA
612 in 0.05% Triton X-100 was pipetted onto the swab (1804-PF, Puritan Medical) and
613 dried at room temperature in an air-clean chamber (825-PCR/HEPA, Plas-Labs,
614 Lansing, NI) for 4 hours before packaging in a sealed foil pouch with desiccant (S-
615 8032, ULINE). The unified sampler was built from parts using an assembly jig
616 (custom order from Hygiena, LLC, Camarillo, CA). The unified dispenser contained a
617 hollow-shaft polyurethane swab attached to a bulb preloaded with 400µL 1x
618 rehydration buffer and a separate tube with a filter and drip dispenser friction fit
619 inside the tube. Each custom sampler kit contained an in-house assembled dispenser
620 unit and one lyophilized RT-LAMP reagent tube.
621
622 **Usability study**
623 The Harmony usability study was approved by the Institutional Review Board at the
624 University of Washington (IRB#: STUDY00010884), and informed consent was
625 provided by participants. HCWs (*n = 10*), including registered nurses, medical
626 students, and dental students were enrolled in this study over the course of 1 month.
627 All data was collected without identifiers. The primary objective of this study was to
628 determine the accuracy and precision of the two sample transfer methods and test if
629 variation in reproducibility impacted assay performance, and the secondary objective
630 was to gather user input on the feasibility of each protocol. Participants first received
631 an explanation of the test and its intended use, then watched an instructional video
632 narrated by the facilitator to become familiar with the Harmony workflow (**Movie S1**
633 **and Movie S2**). After watching the video, participants were given a packet with a
634 unique identifier that contained comprehensive instructions for the study procedures
635 and survey questions. Study procedures were modeled on a coaching methodology
636 (*40*) to allow natural progression of the procedures and to identify blocking steps in
637 the instructions. The facilitator sat 10 feet from the participant and kept a record of
638 verbal questions and comments from participants but did not provide answers to
639 procedural questions unless the participant could not proceed.
640

641 For part 1, data related to user preference on sample preparation, tube sizes, and their
642 level of confidence in performing each task were collected anonymously as prompts
643 within their study packet. Open-ended questions were extracted for themes in errors
644 or issues and supplemented with comments and observations recorded by the
645 facilitator. Samples were saved with de-identified labels, and after all participants had
646 completed the study facilitators measured volumes in each receiving tube from part 1.
647 The variances of the volume recovered by each method were tested for their equality
648 using F-Test, and the P-value was reported. The means of the recovered volumes
649 transferred by LPs or HCWs were compared using Student's *t*-test (two-sided), and
650 the *p*-value was reported.
651
652 For part 2, each participant followed instructions in the packet and on the integrated
653 mobile phone to complete the entire Harmony workflow on four total contrived
654 samples (two samples using the transfer pipette protocol and two using the unified
655 sampler system). Kits were prepared as specified above.
656
657 The lab personnel ($n = 5$) portion of the user testing aimed to compare performance of
658 the Harmony device by HCW to that of an "experienced" population, by replicating
659 this process with four students and a researcher from the Lutz Lab. Survey questions
660 were omitted for this group because these volunteers provided feedback throughout
661 the development of Harmony and their views are included in the discussion of this
662 manuscript. The accuracies of tests performed by LPs and HCWs using each method
663 were tested for their equality using *Z*-test (two-sided), and the *p*-value was reported.
664
665 **Clinical nasal swab specimens from individuals presenting respiratory symptoms**
666 A minimum sample size of 30 (each negative and positive) was required to achieve
667 the confidence interval (**CI**) of 90 -100% (binomial cumulative distribution function)
668 should all results be accurate. Our clinical specimen panel ($n = 110$) was previously
669 used to evaluate other SARS-CoV-2 assays (*35*), but 9 specimens had insufficient
670 volume for RNA extraction and were thus excluded from the study. These specimens
671 were collected with informed consent as part of the Seattle Flu Study, approved by the
672 Institutional Review Board at the University of Washington (IRB#: STUDY0006181).
673 Thermo Fisher's OpenArray is an arrayed RT-qPCR system capable of detecting up to
674 26 pathogens simultaneously in a semi-quantitative manner. Specimens from the
675 Seattle Flu Study that had other respiratory pathogens detected using the OpenArray
676 platform were used to determine cross reactivity with Harmony. All participant
677 specimens were de-identified prior to the transfer to the Lutz Lab at the University of
678 Washington for analysis. The remaining 101 specimens were evaluated using the
679 newly extracted RNA for analysis by RT-qPCR and Harmony system, to avoid
680 variations introduced from different batches of extraction. RNA was extracted
681 from clinical nasal swab specimens stored in viral transport media using
682 the QIAamp Viral RNA Mini Kit (52906; Qiagen, Hilden, Germany). Prior to
683 extraction, 100µL of each specimen was mixed with 40µL negative VTM to reach the
684 suggested 140µL sample volume. RNA was extracted according to the manufacturer's
685 protocol, eluted into 70µL of EB buffer, and stored at -80°C in single-use aliquots
686 until amplification. 5µL of RNA was used for analysis in 20µL RT-qPCR using U.S.
687 CDC N1, N2, or RP human control assays (*23*). 10µL of RNA was used for analysis
688 in 40µL lyophilized RT-LAMP in the Harmony workflow. Each sample was run in
689 duplicate. Only samples with positive results from both Harmony replicates were
690 reported as positive for SARS-CoV-2. Sensitivity (TP/(TP + FN)), specificity

691 (TN/(TN+FP)), and concordance ((TP+TN)/(TP+TN+FP+FN)) were calculated and
692 reported with 95% CI using binomial exact proportions.
693
694 **XPRIZE contrived sample panel**
695 The blinded panel was assembled and distributed by HudsonAlpha Discovery
696 (Huntsville, AL) for the COVID-19 XPRIZE competition, and information on the
697 samples was revealed to the authors only after results were submitted to XPRIZE.
698 Samples were shipped to the Lutz Lab at the University of Washington. We reported
699 results for contrived samples of chemically inactivated SARS-CoV-2 viral particle
700 (ZeptoMetrix Corporation, Buffalo, NY) spiked in phosphate-buffered saline (**1x**
701 **PBS**) (*n = 29*), nasal specimens (*n = 20*), or saliva (*n = 20*) at 0 to 1000
702 copies/reaction. All samples came in liquid form. We added 10µL sample and 30µL
703 Harmony rehydration buffer to rehydrate each lyophilized reagents and tested across 7
704 different Harmony devices. Each sample was originally tested once for each sample.
705 To affirm the identity of these specimens, we also performed RT-qPCR using CDC
706 primer/probes after the samples had been tested using the Harmony system. To
707 improve our confidence in reporting sensitivity and specificity, we tested two
708 additional replicates for each sample to achieve a total of triplicates.
709
710 **Housing**
711 The housing combines the heater/reader assembly with the cell phone, while
712 concealing the connector cables and presenting a sturdy and easy-to-use platform. The
713 3D CAD program, Fusion 360 (AutoDesk), was used for the design of housing.
714 Prototypes were printed in PLA plastic (Overture™ Filament, OVPLA175) using a
715 Prusa i3 MK3s at 0.3mm layer height. Power was supplied to both the heater/reader
716 assembly and the phone simultaneously using a Charge-Plus USB-C (LAVA
717 Computer Manufacturing Inc.) connector device and a standard fast-charging
718 American cellphone charger. The LAVA device also facilitates the transfer of data
719 between the devices.
720
721
722 **Reader/heater device**
723 The aluminum block to house the reagent tubes was custom-made by Bryan
724 Willman according to the specifications in **Fig. S3**. The circuit boards were designed
725 using Autodesk Eagle (San Rafael, CA), and the assembly of the circuit boards are
726 shown in **Fig. S4** and **Fig. S5**. The lid, latch, and upper and lower housing of the
727 device were drawn using SolidWorks (Dassault Systèmes, Waltham, MA) and printed
728 by Xometry - HP MultiJet Fusion 3D (Gaithersburg, MD). All parts were assembled
729 as shown in **Fig. S6**.
730
731 **Real-time fluorescence signal analysis**
732 After the user inserts the reaction tube into the device, the software adjusts the
733 temperature to re-equilibrate the temperature of heat block back to the reaction
734 temperature. During this initial period, the signals from the photo diodes (the blue
735 LED (FAM signal for target amplification) and the yellow LED (TEX 615 signal for
736 the IAC amplification)) are collected but not used in analyses. Once the initial period
737 is over, signal analysis commences. Each signal is analyzed in real time by comparing
738 the current mean of the signal over the most recent 60s interval to the signal's
739 behavior some 360s in the past. Specifically, the current mean is compared to a bound
740 consisting of the signal's mean over the period from 420s to 360s in the past plus a

multiple (1.9x for target, 1.5x for IAC) of the signal's sample standard deviation over that same period. If the current mean exceeds the bound, and maintains that condition for at least 15s, the signal is said to have "indicated". If the signal from the target emission indicates, the presence of SARS-CoV-2 has been detected, and the software immediately reports "positive COVID-19". If the signal from the IAC emission indicates, successful amplification of the IAC has been detected. Then, if the target emission does not also indicate before the end of the run, then a "negative COVID-19" result is reported; this delay in reporting negative results provides the maximum opportunity to detect low concentrations of SARS-CoV-2 that may be present in samples. If neither the target emission nor the IAC emission is detected, "test failed" is reported.

References

1. D. Cucinotta, M. Vanelli, WHO Declares COVID-19 a Pandemic. *Acta bio-medica : Atenei Parmensis* **91**, 157-160 (2020).
2. World Health Organization, 2021, "WHO Coronavirus (COVID-19) Dashboard." 10 August, 2021 https://covid19.who.int/.
3. A. Sandford, 2020, "Coronavirus: Half of humanity now on lockdown as 90 countries call for confinement." Euronews, 10 August, 2021 https://www.euronews.com/2020/04/02/coronavirus-in-europe-spain-s-death-toll-hits-10-000-after-record-950-new-deaths-in-24-hou.
4. G. Bonaccorsi *et al.*, Economic and social consequences of human mobility restrictions under COVID-19. *Proc Natl Acad Sci U S A* **117**, 15530-15535 (2020).
5. R. A. Teran *et al.*, Postvaccination SARS-CoV-2 Infections Among Skilled Nursing Facility Residents and Staff Members - Chicago, Illinois, December 2020-March 2021. *MMWR. Morbidity and mortality weekly report* **70**, 632-638 (2021).
6. C. M. Brown *et al.*, 2021, "Outbreak of SARS-CoV-2 Infections, Including COVID-19 Vaccine Breakthrough Infections, Associated with Large Public Gatherings — Barnstable County, Massachusetts, July 2021." US CDC, 10 August, 2021 https://www.cdc.gov/mmwr/volumes/70/wr/mm7031e2.htm?s_cid=mm7031e2_w#contribAff.
7. Centers for Disease Control and Prevention, 2021, "Requirement for Proof of Negative COVID-19 Test or Recovery from COVID-19 for All Air Passengers Arriving in the United States." 10 August, 2021 https://www.cdc.gov/coronavirus/2019-ncov/travelers/testing-international-air-travelers.html.
8. E. Kline *et al.*, 2021, "Multiplex target-redundant RT-LAMP for robust detection of SARS-CoV-2 using novel fluorescent universal displacement probes." medRxiv, (2021)
9. V. L. Dao Thi *et al.*, A colorimetric RT-LAMP assay and LAMP-sequencing for detecting SARS-CoV-2 RNA in clinical samples. *Sci Transl Med* **12**, (2020).
10. S. Wu *et al.*, Colorimetric isothermal nucleic acid detection of SARS-CoV-2 with dye combination. *Heliyon* **7**, e06886 (2021).
11. J. Xu *et al.*, Room-temperature-storable PCR mixes for SARS-CoV-2 detection. *Clin Biochem* **84**, 73-78 (2020).
12. N. Panpradist *et al.*, OLA-Simple: A software-guided HIV-1 drug resistance test for low-resource laboratories. *EBioMedicine* **50**, 34-44 (2019).
13. N. Panpradist *et al.*, Near point-of-care, point-mutation test to detect drug resistance in HIV-1: a validation study in a Mexican cohort. *AIDS*, (2020).

14. J. Vrana *et al.*, OLA Simple v 1.0: observational study of an app-guided HIV drug resistance test at the Coptic Hope Center in Kenya. *medRxiv*, (2021).
15. B. Moon, M. Jones, J. Valdez, 2003, "Lyophilized beads containing mannitol." Cepheid, 10 August, 2021 https://patents.google.com/patent/US20050069898A1/en.
16. D.-C. Nyan *et al.*, Rapid Detection of Hepatitis B Virus in Blood Plasma by a Specific and Sensitive Loop-Mediated Isothermal Amplification Assay. *Clinical Infectious Diseases* **59**, 16-23 (2014).
17. A. N. Spiess, N. Mueller, R. Ivell, Trehalose is a potent PCR enhancer: lowering of DNA melting temperature and thermal stabilization of taq polymerase by the disaccharide trehalose. *Clin Chem* **50**, 1256-1259 (2004).
18. Y. Mori, K. Nagamine, N. Tomita, T. Notomi, Detection of loop-mediated isothermal amplification reaction by turbidity derived from magnesium pyrophosphate formation. *Biochem Biophys Res Commun* **289**, 150-154 (2001).
19. K. Tone, R. Fujisaki, T. Yamazaki, K. Makimura, Enhancing melting curve analysis for the discrimination of loop-mediated isothermal amplification products from four pathogenic molds: Use of inorganic pyrophosphatase and its effect in reducing the variance in melting temperature values. *J Microbiol Methods* **132**, 41-45 (2017).
20. S. Xie, Y. Yuan, Y. Chai, R. Yuan, Tracing Phosphate Ions Generated during Loop-Mediated Isothermal Amplification for Electrochemical Detection of Nosema bombycis Genomic DNA PTP1. *Anal Chem* **87**, 10268-10274 (2015).
21. I. New England Biolabs, 2021, "Thermostable Inorganic Pyrophosphatase." 10 August, 2021 https://www.neb.com/products/m0296-thermostable-inorganic-pyrophosphatase#Product%20Information.
22. T. Lennox, B. E. Slatko, L. E. Sears, 1995, "Purified thermostable inorganic pyprophosphatase obtainable from thermococcus litoralis " New England Biolabs Inc, 19 August, 2021 https://patents.google.com/patent/US5861296A/en.
23. U.S. Centers for Disease Control and Prevention, 2020, "CDC 2019-Novel Coronavirus (2019-nCoV) Real-Time RT-PCR Diagnostic Panel For Emergency Use Only." U.S. Food and Drug Administration, 10 August, 2021 https://www.fda.gov/media/134922/download.
24. C. Thermo Fisher Scientific, 2021, "OpenArray Technology Overview." 10 August, 2021 https://www.thermofisher.com/us/en/home/life-science/pcr/real-time-pcr/real-time-openarray/open-array-technology.html.
25. C. B. F. Vogels *et al.*, SalivaDirect: A simplified and flexible platform to enhance SARS-CoV-2 testing capacity. *Med (N Y)* **2**, 263-280.e266 (2021).
26. R. Wolfel *et al.*, Virological assessment of hospitalized patients with COVID-2019. *Nature* **581**, 465-469 (2020).
27. J. Zhu, J. Guo, Y. Xu, X. Chen, Viral dynamics of SARS-CoV-2 in saliva from infected patients. *J Infect* **81**, e48-e50 (2020).
28. B. Pang *et al.*, Isothermal Amplification and Ambient Visualization in a Single Tube for the Detection of SARS-CoV-2 Using Loop-Mediated Amplification and CRISPR Technology. *Analytical Chemistry* **92**, 16204-16212 (2020).
29. P. Craw, W. Balachandran, Isothermal nucleic acid amplification technologies for point-of-care diagnostics: a critical review. *Lab Chip* **12**, 2469-2486 (2012).
30. E. Gonzalez-Gonzalez *et al.*, Colorimetric loop-mediated isothermal amplification (LAMP) for cost-effective and quantitative detection of SARS-CoV-2: the change in color in LAMP-based assays quantitatively correlates with viral copy number. *Anal Methods* **13**, 169-178 (2021).

31. J. Rodriguez-Manzano *et al.*, Handheld Point-of-Care System for Rapid Detection of SARS-CoV-2 Extracted RNA in under 20 min. *ACS Cent Sci* **7**, 307-317 (2021).
32. Chaibio. (Santa Clara, CA).
33. W. Putri, D. J. Muscatello, M. S. Stockwell, A. T. Newall, Economic burden of seasonal influenza in the United States. *Vaccine* **36**, 3960-3966 (2018).
34. Centers for Diseases Control and Prevention. (2012).
35. N. Panpradist *et al.*, Simpler and faster Covid-19 testing: Strategies to streamline SARS-CoV-2 molecular assays. *EBioMedicine* **64**, 103236 (2021).
36. G. Gulati *et al.*, Inexpensive workflow to enable simultaneous monitoring of HIV viral load and detection of SARS-CoV-2 infection. *medRxiv*, (2021).
37. N. Morant, University of Bath, (2015).
38. Addgene, "Ligation Independent Cloning." 8 April, 2021 https://www.addgene.org/protocols/lic/.
39. N. Panpradist *et al.*, Swab sample transfer for point-of-care diagnostics: characterization of swab types and manual agitation methods. *PLoS One* **9**, e105786 (2014).
40. R. Mack, J. B. Robinson, in *The Psychology of Expertise,* H. R.R., Ed. (Springer, New York, NY, 1992), pp. 245-268.
41. FPbase, 2021, "Spectra viewer." 20 June, 2020 https://www.fpbase.org/spectra/.
42. Newport, 2021, "Optical Filters." 4 March, 2021 https://www.newport.com/c/optical-filters.
43. Mousers Electronics, 2021, "LED lighting." 4 March, 2021 https://www.mouser.com/Optoelectronics/LED-Lighting/_/N-74g9t.
44. A. Alekseenko *et al.*, Direct detection of SARS-CoV-2 using non-commercial RT-LAMP reagents on heat-inactivated samples. *Sci Rep* **11**, 1820 (2021).
45. B. A. Rabe, C. Cepko, SARS-CoV-2 detection using isothermal amplification and a rapid, inexpensive protocol for sample inactivation and purification. *Proc Natl Acad Sci U S A* **117**, 24450-24458 (2020).
46. S. Wei *et al.*, Direct diagnostic testing of SARS-CoV-2 without the need for prior RNA extraction. *Sci Rep* **11**, 2402 (2021).
47. L. Bokelmann *et al.*, Point-of-care bulk testing for SARS-CoV-2 by combining hybridization capture with improved colorimetric LAMP. *Nat Commun* **12**, 1467 (2021).
48. W. Yamazaki, Y. Matsumura, U. Thongchankaew-Seo, Y. Yamazaki, M. Nagao, Development of a point-of-care test to detect SARS-CoV-2 from saliva which combines a simple RNA extraction method with colorimetric reverse transcription loop-mediated isothermal amplification detection. *J Clin Virol* **136**, 104760 (2021).
49. J. Qian *et al.*, An enhanced isothermal amplification assay for viral detection. *Nat Commun* **11**, 5920 (2020).
50. M. Patchsung *et al.*, Clinical validation of a Cas13-based assay for the detection of SARS-CoV-2 RNA. *Nat Biomed Eng* **4**, 1140-1149 (2020).
51. J. Joung *et al.*, Point-of-care testing for COVID-19 using SHERLOCK diagnostics. *medRxiv*, (2020).
52. J. P. Broughton *et al.*, CRISPR-Cas12-based detection of SARS-CoV-2. *Nat Biotechnol* **38**, 870-874 (2020).
53. I. Mammoth Biosciences, 2020, "INSTRUCTIONS FOR USE SARS-CoV-2 DETECTRTM Reagent Kit." 10 August, 2021 https://www.fda.gov/media/141765/download.

54. UCSF Health Clinical Laboratories UCSF Clinical Labs at China Basin, 2020, "SARS-CoV-2 RNA DETECTR Assay " 10 August, 2021 https://www.fda.gov/media/139937/download.
55. I. MobileDetect Bio, 2020, "MobileDetect-BIO BCC19 Test Kit for SARS-CoV-2 Detection." 2021, 10 August, 2021 https://www.fda.gov/media/141791/download.
56. I. MobileDetect Bio. (2021), vol. 2021.
57. SEASUN BIOMATERIALS Inc., 2021, "AQ-TOP™ COVID-19 Rapid Detection Kit PLUS." 10 August, 2021 https://www.fda.gov/media/142800/download.
58. I. Sherlock Biosciences, 2021, "INSTRUCTIONS FOR USE SherlockTM CRISPR SARS-CoV-2 kit." 10 August, 2021 https://www.fda.gov/media/137746/download.
59. I. Color Health, 2021, "Color SARS-CoV-2 RT-LAMP Diagnostic Assay EUA Summary." 10 August, 2021 https://www.fda.gov/media/138249/download.
60. Lucira Health, 2021, "Lucira™ CHECK-IT COVID-19 Test Kit." 10 August, 2021 https://www.fda.gov/media/147494/download.
61. D. MitraIvan, K. Dimov, J. R. Waldeisen, 2015, "Colorimetric Detection of Nucleic Acid Amplification." 10 August, 2021 https://patents.google.com/patent/US20170044599A1/pt-pt.

Acknowledgments

We thank Bryan Willman for his support in fabricating customized heat blocks, Jan Gray for his help with firmware development, Tom Blank for sharing the PCB fabrication resources, and Dr. Liz Sanocki for the useful feedback on the software user interface. We thank Shawna Cooper for sharing the graphics and content used in Audere's mobile app's flu@home, which influenced the design of the first few screens of the Harmony COVID-19 software. We thank Dr. Paul Yager and Steven Bennett for use of their optical filters during the initial stage of device development. We thank Jason Tauscher at the Washington Nanofabrication Facility for his assistance in cutting the plastic sheet filters. The Washington Nanofabrication Facility is a National Nanotechnology Coordinated Infrastructure (NNCI) site at the University of Washington with partial support from the National Science Foundation via awards NNCI-2025489 and NNCI-1542101. We thank Seattle Flu Study researchers Dr. Jay Shendure and Dr. Jase Gehring for their helpful technical discussion. We thank Dr. Syamal Raychaudhuri, Dr. Frances Chu from Inbios International, and Dr. Gwong-Jen J. Chang for the stimulating discussion. We thank the Seattle Flu Study and the Seattle Coronavirus Assessment Network (SCAN) teams led by Principal Investigators: Helen Y. Chu, MD, MPH, Michael Boeckh, MD, PhD, Janet A. Englund, MD, Michael Famulare, PhD, Barry R. Lutz, PhD, Deborah A. Nickerson, PhD, Mark J. Rieder, PhD, Lea M. Starita, PhD, Mathew Thompson, MD, MPH, DPhil, Jay Shendure, MD, PhD and Trevor Bedford, PhD for providing specimens for testing.

Funding: This work was supported by the Seattle Flu Study (funded by Gates Ventures) and the National Institutes of Health (R01AI140845; 5R61AI140460-03). We thank the Washington Entrepreneurial Research Evaluation and Commercialization HUB program (WE-REACH, U01 HL152401) and their matching grant partners for partly supporting reagents, supplies, and personnel. ITH was

supported in part by the National Institute of General Medical Sciences of the National Institutes of Health under Award Number T32GM008268.
This work does not reflect the views of the funders. The funders were not involved in the design of the study, and funders do not have any ownership over the management and conduct of the study, the data, or the rights to publish.

Author contributions: NP developed lyophilized RT-LAMP and outlined the overall plan for experiments and data visualization presented in this manuscript. RGA developed a mobile software application for operating the device and analyzing results in real-time. MR developed the heater and fluorescent reader device. EK designed the RT-LAMP assay primers and probes and engineered polymerase. EK, ITH and QW synthesized polymerase and provided usability feedback during the development of the Harmony COVID-19 system. ITH and QW prepared *in vitro* RNA transcripts. JHK and VL led the usability study. NP, AKO, and CB tested clinical and contrived specimens. RGA, NP, AKO, SDG, and JHK analyzed the data. ITH and QW prepared the kits and blinded mock samples for usability testing. DL developed housing units to integrate the cell phone, sample preparation station, and the device. LMS and PDH designed and characterized the clinical specimen panel used in this study. PKD provided technical insights. MT oversaw the usability study. BRL oversaw the development and evaluation of the Harmony COVID-19 system. All authors contributed to writing this manuscript and approved the final version.

Competing interest: Provisional patent applications have been filed on several components of the Harmony COVID-19 system. NP, RGA, MR, EK, QW, ITH, DL, and BRL are inventors on one or more provisional patent applications. NP, RGA, MR, EK, QW, ITH, JHK, AKO, CB, DL, and BRL hold equity in a startup company that has licensed related technology and supports ongoing work in the BRL laboratory at the University of Washington but played no role in the study. MT is on the Advisory Board for Visby Medical which produces tests for COVID-19 and has received reimbursement for this work. He has also received reimbursement for medical advice to Roche Molecular Diagnostics and Inflammatix.

Data and materials availability: All data are presented in the main text and supplementary information.

Code availability: Sequence alignment and primer design was performed using Geneious 8.1.9 (Auckland, New Zealand). CFX Maestro (Bio-Rad, Hercules, CA) was used to analyze the RT-PCR results. TapeStation Software (Agilent, Santa Clara, CA) was used to visualize fragments of synthetic RNA. A provisional patent application was filed regarding aspects of the cell phone application. The data analysis algorithm is described in the manuscript.

Figures and Tables

Fig. 1 Harmony COVID-19 workflow, analytical performance, and interpretation.

(**A**) User workflow. A nasal swab is collected and eluted in the rehydration buffer using either a unified sampler-dispenser (shown) or a tube-and-bulb method (**Fig. 8**). The swab eluate is then transferred into the reaction tube to rehydrate lyophilized, pre-loaded RT-LAMP reagents. Users follow the instructions on the cell phone app to record the sample identity, insert the tube in the test slot, and close the device. Four samples can be analyzed in parallel. (Photo credits: (A)1-(A)4, Mark Stone at the University of Washington and (A)5, Christopher Snyder at North Seattle College). (**B**) Examples of on-device analysis. Lyophilized reagents were rehydrated with the eluate from swabs spiked with 0, 200, 2000, or 20,000 copies of SARS-CoV-2 RNA, run on the device, and analyzed in real-time. The samples with SARS-CoV-2 RNA at 2000, 200, and 20 copies/reaction (**rxn**) were reported as positive by software at 27 min, 30 min, and 41 min, respectively; after 60 min the NTC reaction was classified as negative. (**C**) Time-to-result. Individual detection time points ($n = 3$) are plotted. Variation in detection time increases as samples approach the detection limit. (**D**)

1000 Diagnostic algorithm. Harmony COVID-19 software calls samples as positive,
1001 negative, or indeterminate based on detection of the three regions in the nucleocapsid
1002 gene (Harmony NC1 overlapping with the CDC N1 region, Harmony NC2
1003 (overlapping with CDC N3 region excluded from the current kit), and Harmony NC3
1004 overlapping with the CDC N2 region) and the engineered IAC sequence.
1005

1006

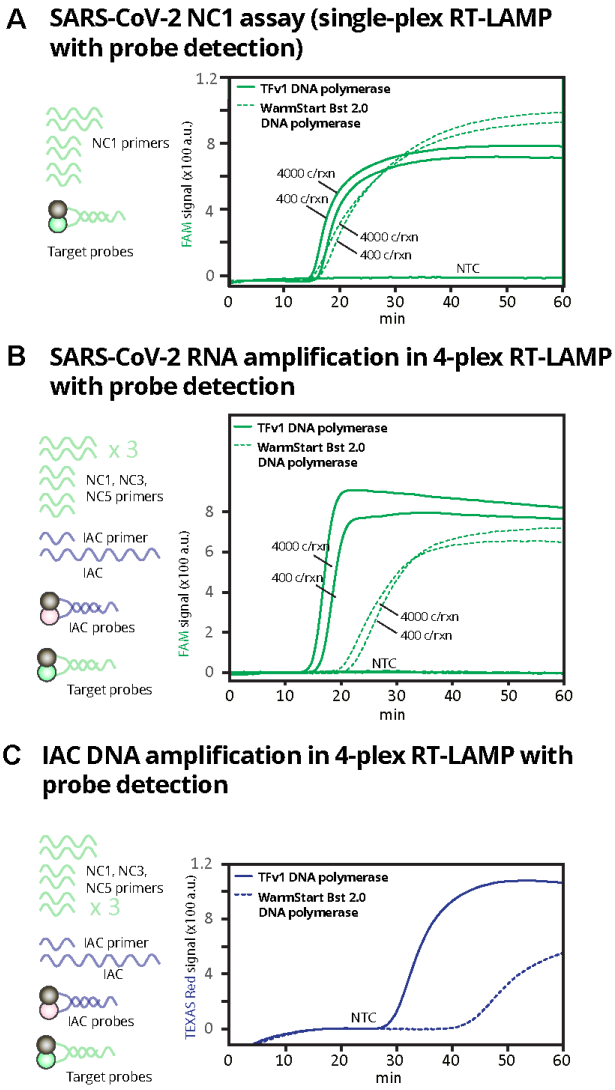

1007
1008 **Fig. 2 Comparison of RT-LAMP using TFv1 polymerase vs commercial Bst**
1009 **polymerase using conventional RT-qPCR machine.** (**A**) FAM signal of the RT-
1010 LAMP assay using fresh reagents (not lyophilized) containing only NC1 primer set (6
1011 primers total) and SARS-CoV-2 detection probe and quencher with 0, 400, or 4000
1012 SARS-CoV-2 RNA copies/reaction (corresponding to 0, 100, or 1,000 SARS-CoV-2
1013 RNA copies/µL, respectively). (**B**) FAM signal and (**C**) IAC signal of the 4-plexed
1014 RT-LAMP assay using fresh reagents containing all primers (18 SARS-CoV-2
1015 primers and 1 IAC primer), SARS-CoV-2 detection probe and quencher, and IAC
1016 detection probe and quencher with 0, 400, or 4000 SARS-CoV-2 RNA
1017 copies/reaction (corresponding to 0, 100, or 1,000 SARS-CoV-2 RNA copies/µL,
1018 respectively). For (**C**) only NTC is shown to indicate true negative. All reactions were
1019 incubated at 63.3 °C for 1 hour and read every 13s in commercial thermal cycler.
1020

1021

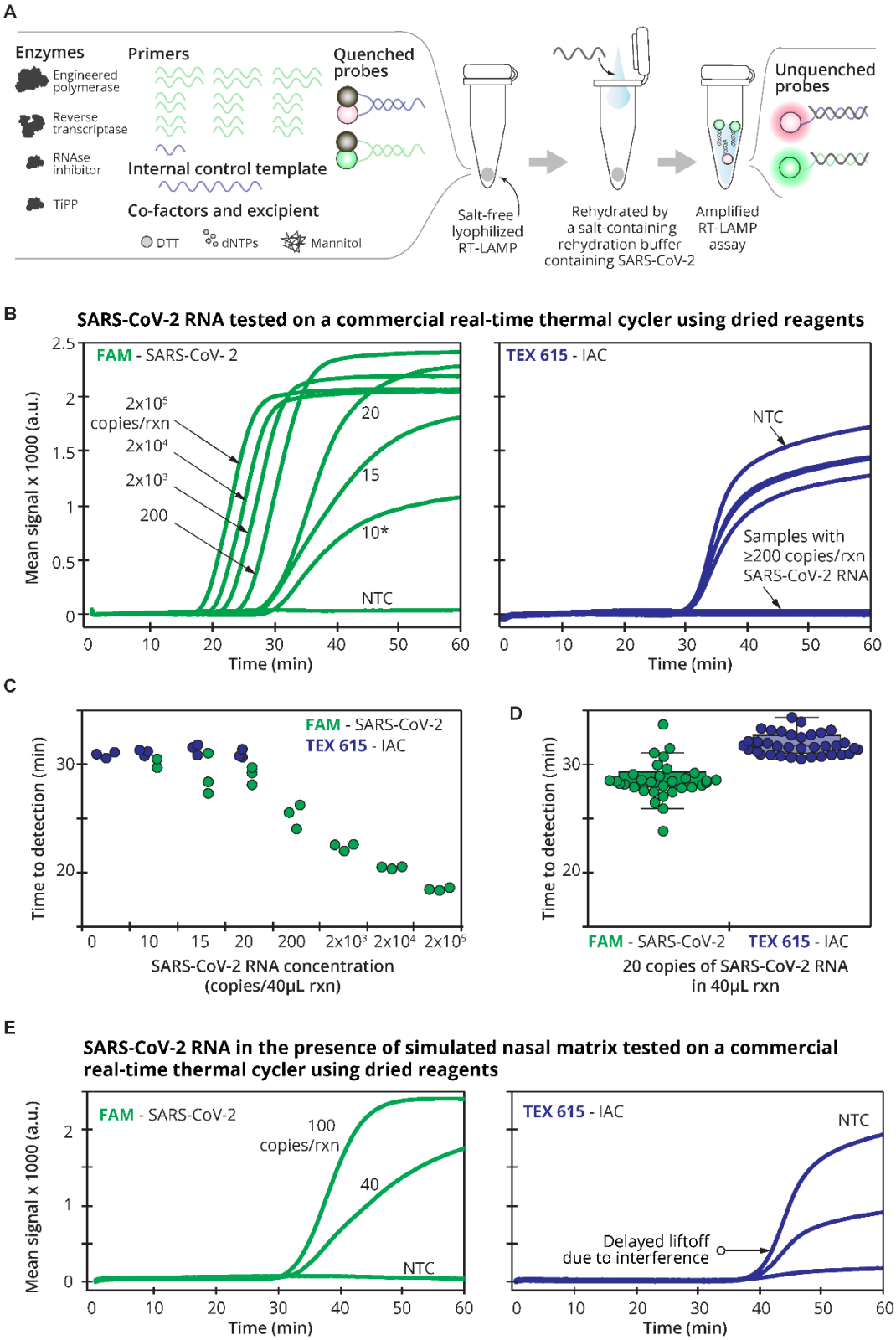

1022
1023
1024 **Fig. 3 Lyophilized RT-LAMP and its analytical sensitivity.**
1025 (**A**) To set up the assay, a sample in elution/rehydration buffer containing
1026 magnesium, Thermopol buffer, and detergents is added to rehydrate the lyophilized
1027 RT-LAMP reagents in a single step. (**B**) Real-time amplification signal of RT-LAMP
1028 reactions containing SARS-CoV-2 RNA (**NTC**; no template control), 10, 15, 20, 200,

2000, $2x10^4$, or $2x10^5$ copies/40µL reaction (**rxn**). The left panel shows the average (*n = 3*) FAM signal detecting SARS-CoV-2. *Only 2/3 replicates of 10 copies/rxn amplified so the average was from duplicate reactions. The right panel shows TEX 615 signal detecting the internal amplification control (IAC). The IAC was detected in the NTC (*n* = 3) and in the single 10 copies/reaction that did not detect SARS-CoV-2. (**C**) Time to detection of SARS-CoV-2 and IAC targets reported by the real-time thermal cycler. Individual data points are plotted. Note that only 2/3 replicates of 10 copies/reaction amplified. IAC signals were properly detected in NTC (*n = 3*) and 1 of the 3 replicates of 10 copies/reaction undetected for SARS-CoV-2. (**D**) Evaluation of analytical sensitivity at 20 copies/reaction of SARS-CoV-2 RNA (*n = 40*), performed in two different runs (*n = 20* each) with two different serially diluted RNA samples. Time-to-result of individual samples are plotted along with medians (middle lines of the boxes), interquartile ranges (edges of the boxes), ranges (the ends of whiskers), and outliers (data points outside the whiskers). (**E**) Impact of nasal matrix. SARS-CoV-2 RNA at 0, 40, or 100 copies/reaction (corresponding to 0, 1, or 2.5 copies/µL) was amplified in lyophilized RT-LAMP in the presence of simulated nasal matrix (*n = 3*). All data was measured every 13s using FAM and TEX 615 channels, by a real-time thermal cycler in 1h reactions at 63.3°C, and (**C**).

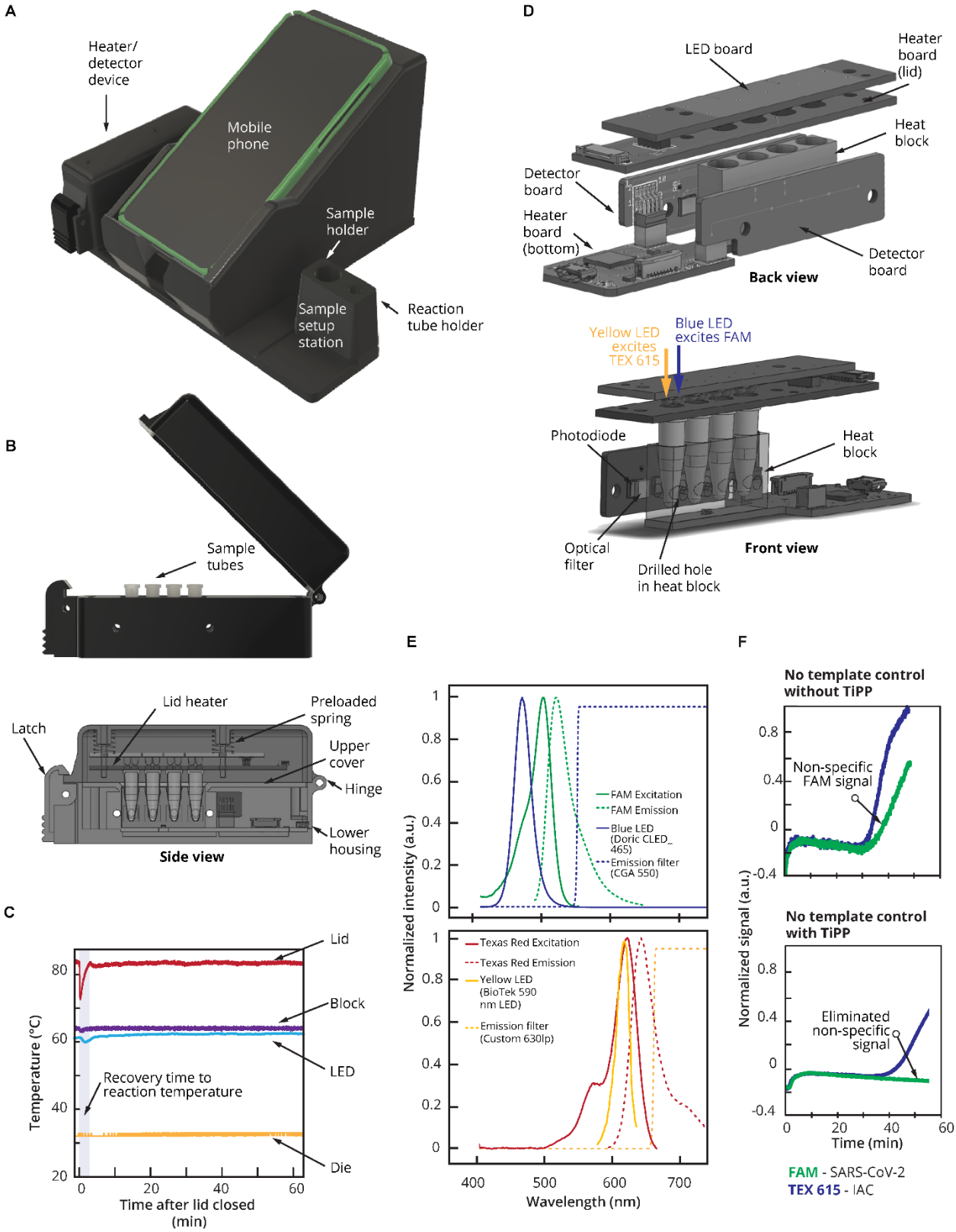

Fig. 4 Overview of Harmony COVID-19 hardware.
(**A**) Plastic case cradles the cell phone (removable and connected by a spring cable), mounts the heater/reader device, and houses a Charge-Plus USB-C connector hub (not

shown). A sample station holds the sample and reaction tube during processing and is detachable to allow cleaning. Weight: 266g housing, 104g heater/reader device (total <0.5kg). Dimensions: 205mm x 167.5mm x 125mm housing, 30mm x 120mm x 50mm heater/reader device. (**B**) The heater/reader device contains an aluminum block with wells for four samples (0.2mL reagent tubes) and is heated from the bottom by a resistive heater made from serpentine conductive traces on a printed circuit board. In the middle of the heater, a temperature sensor (Class B Platinum RTD) is used to measure the heat block temperature. Power to the heater is supplied by a MOSFET and modulated by varying the PWM duty cycle of the MOSFET. (**C**) Temperature profile after the lid opening throughout a 60-min assay run. The microcontroller (die) is measured to ensure the electronics are not overheated. (**D**) Lid heater, LED, and detector. A heater (85°C) on top of the tube prevents condensation on the tube lid. The lid heater is spring loaded to apply a preload force to the tubes to ensure good thermal contact and contains pass-through holes for excitation LEDs. (**E**) Spectral characteristics of the detection system. Blue and yellow LEDs provide excitation for FAM and TEX 615, respectively, and photodetectors on each side detect light passing through emission filters (spectral information from manufacturers(*41-43*)). The LEDs are operated independently (only one LED is illuminated at a given time). (**F**) Effect of thermostable inorganic pyrophosphatase (**TiPP**) on RT-LAMP signal in the Harmony device. Normalized signal of negative control samples using the RT-LAMP formulation with and without TiPP ($n = 1$ each) at 64°C.

Fig. 5 Cell phone user interface and result reporting.
The Android Harmony application guides the user through steps to set up and run the test. (**A**) Intended use of the device. (**B**) Instructions for the user to prepare samples. (**B**) Selection of the number of samples. (**D**) Collection of sample identifiers by barcode, photo capture, or manual typing. (**E**) Instruction to insert the tube when the temperature of the device reaches the reaction temperature. (**F**) Real-time analysis during the test run. (**G**) Positive results are reported as soon as they are detected. (**H**) Negative and IND results are reported at the end of the run time.

1089

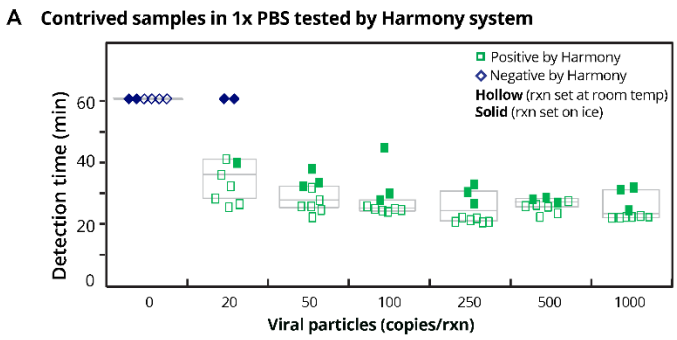

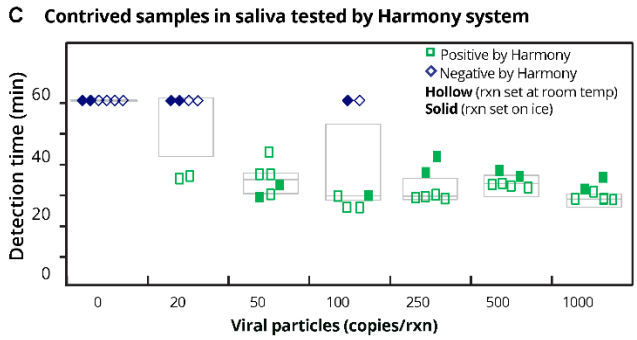

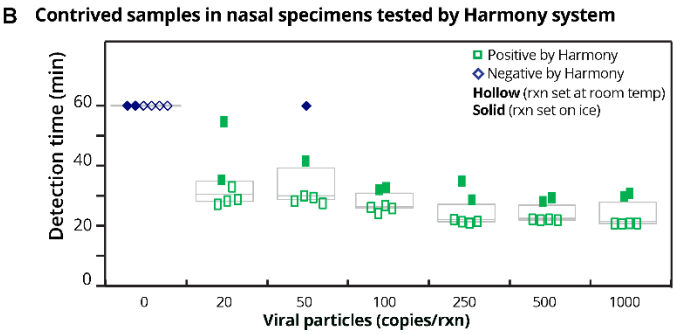

D

Sample matrix	TP	TN	FP	FN	Sensitivity	Specificity
1x PBS	52	6	0	2	**96%** (95%CI: 87-100)	100%
Nasal swabs	35	6	0	1	**97%** (95%CI: 85-100)	100%
Saliva	30	6	0	6	**83%** (95%CI: 67-93)	100%

95% CI (Bionomial Exact)

1090
1091 **Fig. 6** Analysis of XPRIZE contrived sample panel without RNA extraction. (**A**) Viral
1092 particles spiked in 1xPBS were tested in triplicate for each sample (n = 9 total for
1093 positive sample concentrations and n = 6 total for negative samples). (**B**) Viral
1094 particles spiked in human nasal matrix were tested in triplicate (n = 6 total for each
1095 concentration). (**C**) Viral particles spiked in saliva (n = 6 total for each concentration).
1096 (**D**) Summary table for the sensitivity and specificity of the Harmony COVID-19
1097 system on the XPRIZE contrived samples. Concentrations of viral particles are the
1098 final concentrations in each 40uL reaction. Threshold concentration for positive is at
1099 20 viral particle copies/reaction (0.5 copies/µL). Contrived samples below the
1100 positive threshold were also tested (**Fig. S7**). Real-time amplification curves of these
1101 data are in **Fig. S8.** Reactions were set up either at room temperature (*hollow*) or on
1102 ice (*solid*).
1103

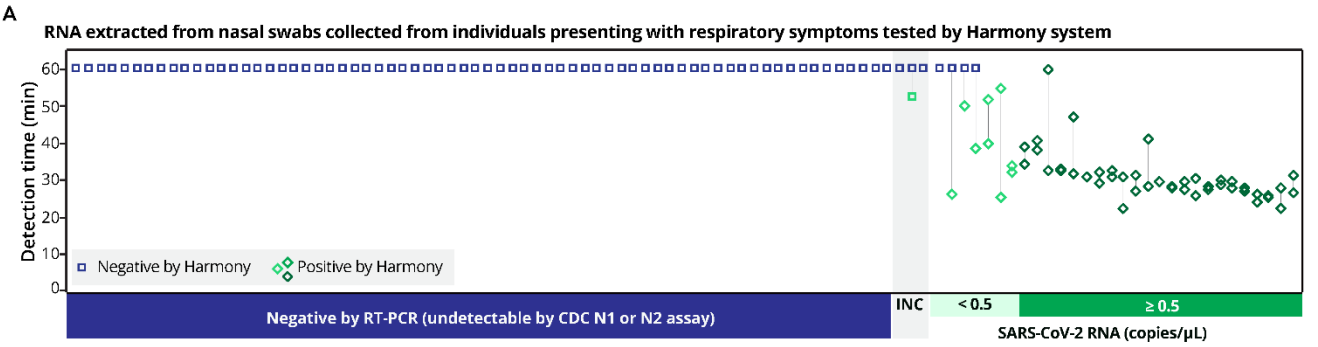

B Summary of Harmony performance on RNA extracted from nasal VTM specimens

Positive thresholds (copies/µL)	TP	TN	FP	FN	Sensitivity	Specificity
> 0	55	136	0	5	92% (95%CI: 82-97)	100% (95%CI: 97-100)
≥ 0.5 (1x LoD)	46	136	0	0	100% (95%CI: 93-100)	100% (95%CI: 97-100)

Counts = no. of tested samples (2 for each specimen); 95%CI (Binomial Exact)

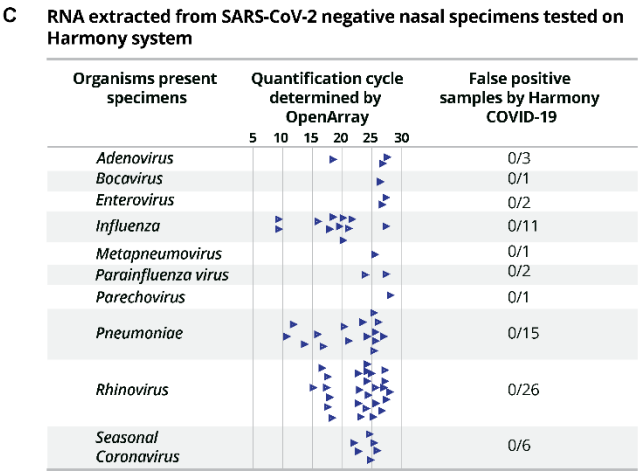
C RNA extracted from SARS-CoV-2 negative nasal specimens tested on Harmony system

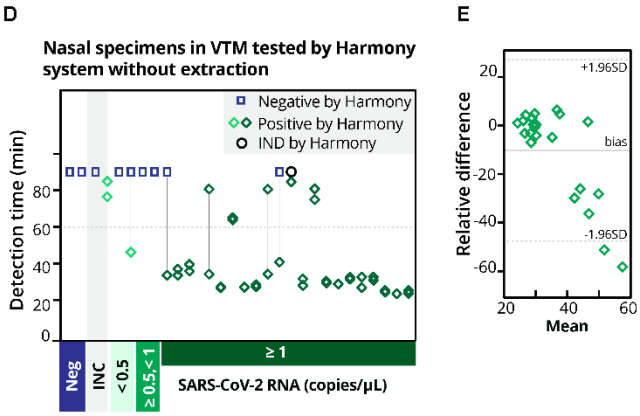
D Nasal specimens in VTM tested by Harmony system without extraction

F Summary of Harmony performance on nasal VTM specimens without extraction

Positive threshold (copies/µL)	TP	TN	FP	FN	IND	Sensitivity
> 0	40	4	0	9	1	82% (95%CI: 68-91)
≥ 0.5 (1x LoD)	39	4	0	6	1	87% (95%CI: 73-95)
≥ 1 (2x LoD)	39	4	0	2	1	95% (95%CI: 83-99)

Counts = no. of tested samples (2 for each specimen); 95%CI (Binomial Exact)

Fig. 7 Harmony COVID-19 performance on clinical specimens.
(**A**) Detection time called by Harmony COVID-19 software for the analysis of purified RNA extracted from human nasal specimens from 101 patients presenting respiratory symptoms. Stored specimens were re-tested by RT-qPCR using N1 and N2 CDC primers; results matched previous results in 30 previous positive specimens (positive for N1 and N2) and 68 previous negative specimens, with three previous positive specimens classified as inconclusive (INC) because they were negative for either CDC N1 or CDC N2 by RT-qPCR. Samples are ranked from left to right by increasing SARS-CoV-2 concentrations as determined by RT-qPCR. Extracted RNA from specimens was analyzed by Harmony COVID-19 (10µL RNA in 40µL RT-LAMP dry reagents, $n = 2$). Samples were classified as positive by Harmony only if both replicates were detected. The classification results by Harmony were compared to RT-qPCR using CDC primers and probes (5µL RNA in 20µL RT-qPCR reaction). (**B**) Organisms in clinical samples collected from individuals presenting with respiratory symptoms were quantified using OpenArray, as previously described(*35*). High quantification cycle values indicate low concentrations. All these specimens

1123 were correctly identified as SARS-CoV-2 negative by Harmony. (**C**) Summary table
1124 for the sensitivity and specificity of the Harmony COVID-19 system using extracted
1125 RNA from clinical specimens (RT-qPCR INC samples excluded). (**D**) Detection time
1126 called by Harmony COVID-19 software for the analysis on 27 VTM specimens
1127 previously tested in (A). Without the RNA extraction step, 10µL VTM was added in
1128 the final 40µL RT-LAMP rxn, ($n = 2$). Dashed line indicates the detection time at 60
1129 min. (**E**) Bland-Altman plot of the detection time of SARS-CoV-2 positive specimens
1130 of the direct VTM group compared to the extracted RNA group. Dashed lines indicate
1131 the acceptable bound of the difference of the detection time (mean ± 1.96SD). (**F**)
1132 Summary table for the sensitivity of the Harmony COVID-19 system using VTM
1133 specimens without extraction.
1134

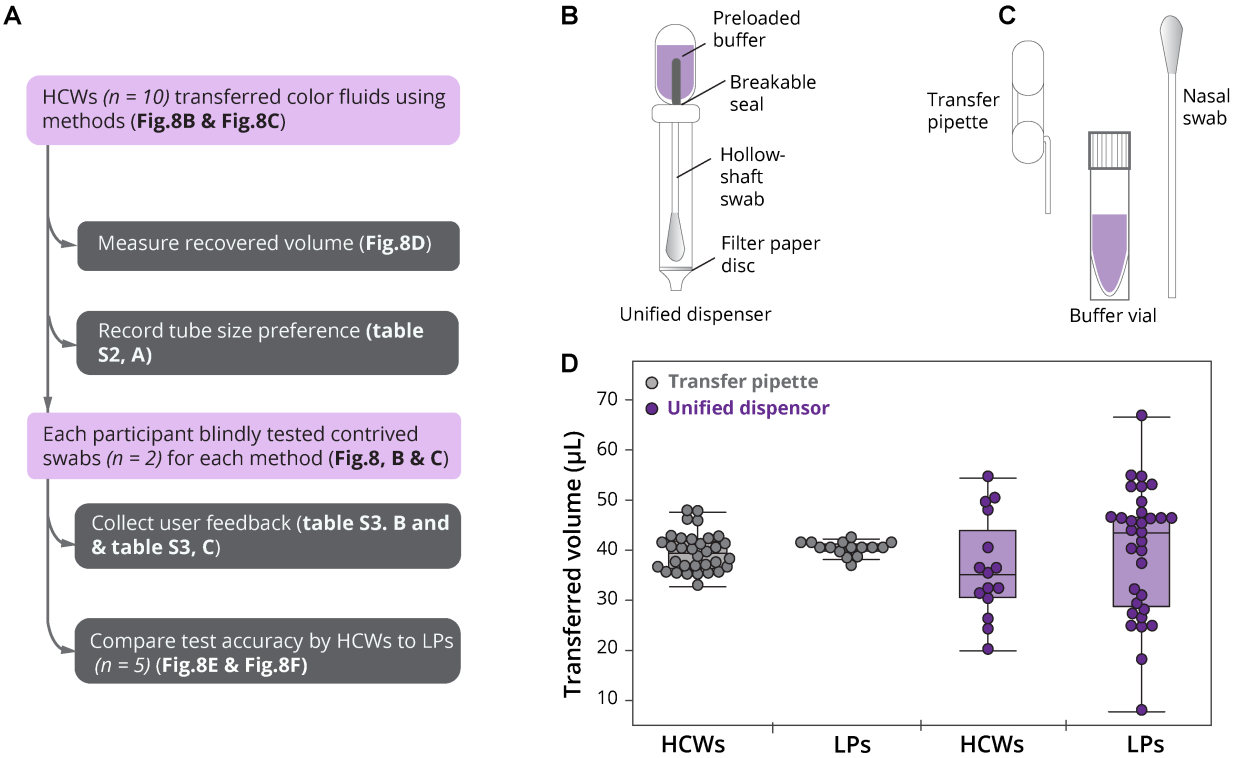

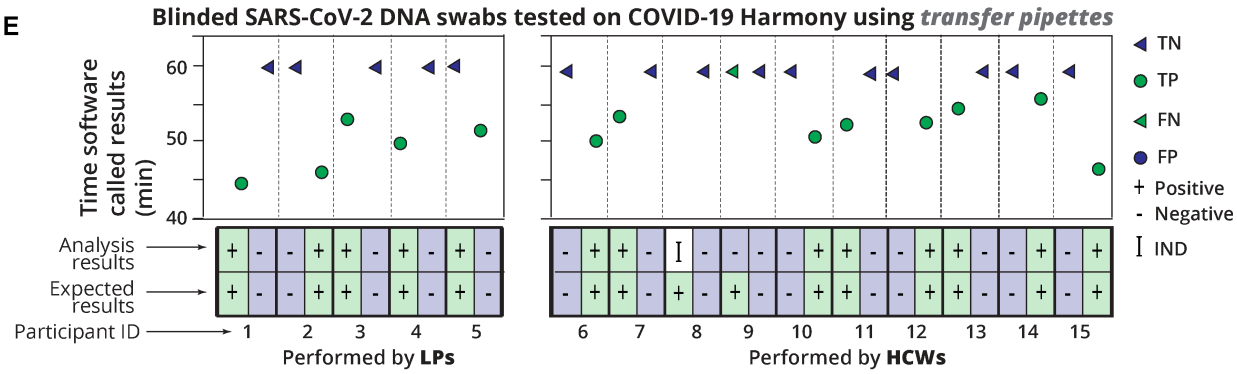

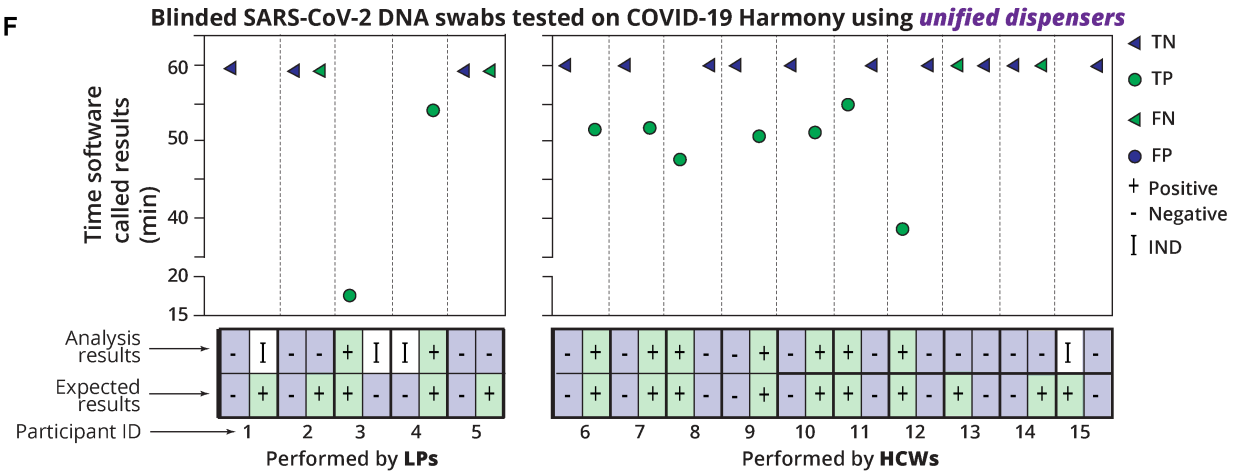

G

	Performance with *transfer pipettes*						
	TP	TN	FP	FN	IND	% Accuracy	% IND
LPs	5	5	0	0	0	100	0
HCWs	9	9	0	1	1	95	5

H

Performance with *unified dispenser*						
TP	TN	FP	FN	IND	% Accuracy	% IND
2	3	0	2	3	71	30
7	10	0	2	1	89	5

1136
1137 **Fig. 8 Usability study of Harmony COVID-19 workflow including two sample**
1138 **transfer methods at the POC**.
1139 (**A**) Study design. (**B**) Illustration of the first sample transfer method option using a
1140 unified dispenser, which integrates a swab, buffer container, and a dropper in a single
1141 device. The contained buffer is released to elute the swab sample by cracking a
1142 conduit, the user agitates the fluid by shaking the tube, and a dropper tip allows the
1143 use to transfer two drops of fluid to the reaction tube by squeezing the body of the
1144 device. (**C**) Illustration of the second sample transfer method including a volumetric
1145 transfer pipette (40µL), a nasal swab, and a pre-loaded buffer vial. **Movie S1**
1146 demonstrates this workflow. Briefly, swabs are manually rubbed on the side of the
1147 tube for 30 seconds, soaked for 1 minute, and removed. The pipette is then used to
1148 transfer the swab eluate to rehydrate the lyophilized RT-LAMP reaction tube. **Movie**
1149 **S2** demonstrates this workflow. (**D**) Volume transferred by each method performed by
1150 healthcare workers (**HCWs**) or laboratory personnel (**LPs**). Individual volume
1151 measurements are plotted along with medians (middle lines of the boxes),
1152 interquartile ranges (edges of the boxes), and ranges (the ends of whiskers). **e** and **f**,
1153 Assay performance on blinded contrived swabs (one negative swab and one positive
1154 swab with SARS-CoV-2 DNA at 1,000 copies/swab, corresponding to 100
1155 copies/reaction) by LPs ($n = 5$) and untrained HCWs ($n = 10$) using transfer pipettes,
1156 (**E**) or unified dispensers, (**F**) The usability experiment written protocol is available
1157 on protocol.io (https://dx.doi.org/10.17504/protocols.io.bkvskw6e) and as a visual
1158 demonstration in **Movie S1 and Movie S2**. (**G**) Performance summary for the transfer
1159 pipette method. (**H**) Performance summary for the unified dispenser method.
1160

1161
1162 **Table 1** Feature comparison between the Harmony COVID-19 system and other assays.
1163 (**A**) Comparison to the U.S. CDC assay.(*23*) Full cost calculations for reagents and devices
1164 are enclosed in **Tables S4** and **Table S5**.
1165

Item	Standard RT-PCR assay (based on the U.S. CDC protocol)(*23*)	Covid-19 Harmony
SARS-CoV-2 primer detection	Separate reactions for N1 and N2	Multi-target redundancy amplifying three regions of the N gene in a single reaction tube
Process control	Human RP gene	Engineered internal control
LoD	1-3.2 copies/µL from extracted RNA	0.5 copies/µL (20 copies/40µL reaction) from synthetic RNA; 1 copies/µL (40 copies/40µL reaction) from extracted RNA from VTM; 2.5 copies/µL (100 copies/40µL reaction) from contrived nasal samples
Consumable cost	$12.94 / sample ($6 extraction kit and $6.94 for three RT-PCR Taq Path/IDT probes)	$8.00 / sample
Easy to use reagents	No	Yes
Batch size	24 specimens	Not required, run up to 4 samples
Equipment cost	> $5000 qPCR machine	$247 customized heater/reader
Time for sample-to-result	260 min Hands-on: 120 min Wait-time: 120 min Interpretation: 20 min	21-91 min Hands-on: 1 min for direct amplification Wait-time: 20-45 min for positive samples, but 90 min is required to confirm true negative

1166 (**B**) Comparison of Harmony COVID-19 to other isothermal assays for SARS-CoV-2.

Published assays	Amplification chemistry	Multi-target redundancy in a single tube	Reported LoD	User-friendly device with ready-to-use reagents and a closed system	Demonstration of use by HCWs
Harmony COVID-19 (This study)	RT-LAMP	Yes	0.5-2.5 copies/µL	Yes	Yes
A Alekseenko *et. al.* 2021(*44*)	RT-LAMP	No	10 copies/µL	No	No
BA Rabe and C Cepko(*45*)	RT-LAMP	No	50 copies/µL	No	No
S Wei, *et. al.*(*46*)	RT-LAMP	No	2.5 copies/µL	No	No
D Thi, *et. al.* (*9*)	RT-LAMP	No	5 copies/µL	No	No
L Bokelmann *et. al.* (*47*)	RT-LAMP	No	5-20 copies/µL	No	No
W Yamaziki *et. al.* (*48*)	RT-LAMP	Yes	25 copies/µL	No	No
J Qian *et. al.*(*49*)	RPA	Yes	0.5 copies/µL	No	No
M Patchsung *et. al.*(*50*)	SHERLOCK	No	2.1 copies/µL	No	No
J Joung *et. al.*(*51*)	SHERLOCK	No	2 copies/µL	No	No
J Broughton *et.al.* (*52*)	CRISPR cas12	No	10 copy/µL	No	No

1167
1168

1169
1170 **Supplementary Materials**
1171 **Table. S1.**
1172 Summary of RT-LAMP based technologies that have received emergency use
1173 authorization as of July 15th, 2021.
1174 **Table. S2.**
1175 Primers, probes, and control sequences.
1176 **Table. S3.**
1177 Feedback from the HCWs
1178 **Table. S4.**
1179 Detailed reagent and device cost at a production scale of 10,000 units.
1180 **Table. S5.**
1181 Consumable costs per test
1182
1183 **Fig. S1.**
1184 Effects of excipients on fresh RT-LAMP reactions tested on a commercial real-time
1185 thermal cycler.
1186 **Fig. S2.**
1187 Cross-reactivity of MERS and SARS in lyophilized RT-LAMP.
1188 **Fig. S3.**
1189 Heat block used in Harmony COVID-19 device.
1190 **Fig. S4.**
1191 The design of optical and heater circuit boards for the Harmony COVID-19 device.
1192 **Fig. S5.**
1193 Circuit board assembly and required parts
1194 **Fig. S6.**
1195 Device assembly
1196 **Fig. S7.**
1197 Analysis of XPRIZE panel of contrived samples containing less than 20
1198 copies/reaction.
1199 **Fig. S8.**
1200 Real-time amplification curves of samples analyzed by HARMONY Covid-19
1201 **Fig. S9.**
1202 Standard curves of RT-qPCR
1203 **Fig. S10.**
1204 Real-time amplification curves of RT-qPCR using CDC primers/probes.
1205
1206 **Video S1** Demonstration of transfer pipette workflow incorporated with Harmony
1207 COVID-19.
1208 **Video S2** Demonstration of the integrated sampling system workflow with Harmony
1209 COVID-19